TISSUE ENGINEERING: Part C
Volume 17, Number 2, 2011
© Mary Ann Liebert, Inc.
DOI: 10.1089/ten.tec.2010.0139

Transplantation of Human Adipose Tissue-Derived Multilineage Progenitor Cells Reduces Serum Cholesterol in Hyperlipidemic Watanabe Rabbits

Hanayuki Okura, Ph.D.,[1,2] Ayami Saga, M.S.,[1] Yuichi Fumimoto, M.D., Ph.D.,[1] Mayumi Soeda, V.M.D.,[1] Mariko Moriyama, Ph.D.,[1,3] Hiroyuki Moriyama, Ph.D.,[3] Koji Nagai, M.D.,[1,4] Chun-Man Lee, M.D., Ph.D.,[1] Shizuya Yamashita, M.D., Ph.D.,[5] Akihiro Ichinose, M.D., Ph.D.,[4] Takao Hayakawa, Ph.D.,[3] and Akifumi Matsuyama, M.D., Ph.D.[1]

Familial hypercholesterolemia (FH) is an autosomal codominant disease characterized by high concentrations of proatherogenic lipoproteins and premature atherosclerosis secondary to low-density lipoprotein (LDL) receptor deficiency. We examined a novel cell therapy strategy for the treatment of FH in the Watanabe heritable hyperlipidemic (WHHL) rabbit, an animal model for homozygous FH. We delivered human adipose tissue-derived multilineage progenitor cells (hADMPCs) via portal vein and followed by immunosuppressive regimen to avoid xenogenic rejection. Transplantation of hADMPCs resulted in significant reductions in total cholesterol, and the reductions were observed within 4 weeks and maintained for 12 weeks. ^{125}I-LDL turnover study showed that the rate of LDL clearance was significantly higher in the WHHL rabbits with transplanted hADMPCs than those without transplanted. After transplantation hADMPCs were localized in the portal triad, subsequently integrated into the hepatic parenchyma. The integrated cells expressed human albumin, human alpha-1-antitrypsin, human Factor IX, human LDL receptors, and human bile salt export pump, indicating that the transplanted hADMPCs resided, survived, and showed hepatocytic differentiation *in vivo* and lowered serum cholesterol in the WHHL rabbits. These results suggested that hADMPC transplantation could correct the metabolic defects and be a novel therapy for inherited liver diseases.

Introduction

Familial hypercholesterolemia (FH) is characterized by premature and accelerated development of atherosclerotic lesions caused by elevated levels of cholesterol-rich lipoproteins in plasma. The disease is caused by mutations in the low-density lipoprotein (LDL) receptor gene that result in a significant decrease in receptor-mediated uptake of lipoproteins from the circulation.[1–3] Patients homozygous for defects in LDL receptors have serum cholesterol levels 5–10 times those of normal and suffer as early as the first two decades of life from complications such as coronary artery disease.[4,5] In homozygous FH patients, conventional drug therapy cannot treat the condition, and therapeutic recourses are limited to chronic plasmapheresis or orthotopic liver transplantation.[1] Although liver transplants lower LDL levels, the procedure is life threatening; in addition, donor livers are in short supply. Cellular transplantation has been proposed to provide functional LDL receptors for the treatment of hypercholesterolemia. Transplantation of allogenic and xenogenic hepatocytes has been shown to be effective in lowering serum cholesterol in the Watanabe heritable hyperlipidemic (WHHL) rabbit,[6–9] which is an animal model for homozygous FH. Further, a number of gene therapy approaches have shown some promises in animal models and human,[10–13] and the therapies will cure a number of patients with FH in near future. As an alternative to whole-organ transplantation and/or gene therapy, we have investigated the ability of human adipose tissue-derived multilineage progenitor cells (hADMPCs) to differentiate into hepatocytes *in vitro* and to replace critical liver functions[14] as well as previous reports,[15,16] because the *in vitro* differentiation of hADMPCs into various kinds of cell types in now well reported and hADMPCs can be easily and safely obtained in large

[1]Department of Somatic Stem Cell Therapy and Health Policy, Foundation for Biomedical Research and Innovation, Kobe, Japan.
[2]Research Fellow of the Japan Society for the Promotion of Science, Tokyo, Japan.
[3]Pharmaceutical Research and Technology Institute, Kinki University, Osaka, Japan.
[4]Department of Plastic Surgery, Kobe University Hospital, Kobe, Japan.
[5]Division of Cardiology, Department of Internal Medicine, Osaka University Graduate School of Medicine, Osaka Japan.

quantities without serious ethics issues.[17,18] In this study, we are investigating whether hADMPCs could differentiate into hepatocytes *in vivo* and replace critical liver functions as considerable therapeutic potential for cellular replacement.

Materials and Methods

Cells

hADMPCs were prepared as described previously[19] with some modifications.[14,17,18] Adipose tissues from human subjects were resected during plastic surgery in five subjects (four males and one female, age, 20–60 years) as excess discards. Ten to 50 g of subcutaneous adipose tissue was collected from each subject. All subjects provided informed consent. The protocol was approved by the Review Board for Human Research of Kobe University Graduate School of Medicine, Osaka University Graduate School of Medicine, and Foundation for Biomedical Research and Innovation. After five to six passages, the hADMPCs were used for transplantation. Human cryopreserved hepatocytes were purchased from Invitrogen (Lot number: HuP81) and cultured as indicated by the manufacturer's protocol. Human adipose tissue-derived fibroblastic cells were obtained according to previous report.[20]

Flow cytometric analysis

hADMPCs isolated from adipose tissue were characterized by flow cytometry. Cells were detached from culture dishes by 0.25% trypsin/ethylenediaminetetraacetic acid (EDTA) and suspended in Dulbecco's phosphate-buffered saline (DPBS; Nacalai Tesque) containing 0.1% fetal bovine serum. Aliquots (5×10^5 cells) were incubated for 30 min at 4°C with fluorescein isothiocyanate-conjugated mouse monoclonal antibodies to human CD31 (BD PharMingen), CD105 (Ancell Corporation), CD133 (R&D Systems), phycoerythrin-conjugated mouse monoclonal antibodies to human CD29, CD34, CD45, CD73 (BD PharMingen), CD44, or CD166 (Ancell). Isotype-identical antibodies served as controls. Further, the cells were incubated with mouse monoclonal antibodies against human stage-specific embryonic antigen-4 (from Chemicon International, Inc.), ABCG-2, or CD117 (BD PharMingen) with nonspecific mouse antibody used as a negative control. After washing with DPBS, cells were incubated with phycoerythrin-labeled goat anti-mouse Ig antibody (BD PharMingen) for 30 min at 4°C. After three washes, cells were resuspended in DPBS and analyzed by flow cytometry using a FACSCalibur flow cytometer and CellQuest Pro software (BD Biosciences).

Adipogenic, osteogenic, and chondrogenic differentiation procedure

For adipogenic differentiation, cells were cultured in the differentiation medium (Zen-Bio, Inc.). After 3 days, half of the medium was changed with adipocyte medium (Zen-Bio) every 2 days. Five days after differentiation, adipocytes were characterized by microscopic observation of intracellular lipid droplets by Oil Red O staining. Osteogenic differentiation was induced by culturing the cells in Dulbecco's modified Eagle's medium containing 10 nM dexamethasone, 50 mg/dL ascorbic acid 2-phosphate, 10 mM β-glycerophosphate (Sigma), and 10% fetal bovine serum. Differentiation was examined by Alizarin red staining. For Alizarin red staining, the cells were washed three times and fixed with dehydrated ethanol. After fixation, the cells were stained with 1% Alizarin red S in 0.1% NH_4OH (pH 6.5) for 5 min and then washed with H_2O. For chondrogenic differentiation, hADMPCs were first trypsinized and 2×10^5 cells were centrifuged at 400 *g* for 10 min. The resulting pellets were cultured in the chondrogenic medium (alpha-minimum essential medium (alpha-MEM) supplemented with 10 ng/mL transforming growth factor-β, 10 nM dexamethasone, 100 μM ascorbate, and 10 μL/mL 100×ITS Solution) for 14 days. For Alcian Blue staining, nuclear counterstaining with Weigert's hematoxylin was followed by 0.5% Alcian Blue 8GX for proteoglycan-rich cartilage matrix.

hADMPC transplantation and immunosuppression regimen

WHHL rabbits (8 weeks old; purchased from Kitayama-labes, Inc.) were anesthetized with pentobarbital (50 mg/kg). An incision distal and parallel to the lower end of the ribcage was made. The peritoneum was incised, and hADMPCs ($n=5$) or human adipose tissue-derived fibroblastic cells ($n=3$) (3×10^7 cells) suspended in 3 mL of Hanks' balanced salt solutions (HBSS) (20°C) or 3 mL of control saline ($n=6$) were infused in 5 min into the portal vein via a 18-gauge Angiocath™ (BD). The immunosuppression regimen (Fig. 1A) consisted of the following: (1) intramuscular injection of cyclosporin A (6 mg/kg/day) daily from the day before surgery to sacrifice; (2) intramuscular injection of rapamycin (0.05 mg/kg/day) daily from the day before surgery to sacrifice; (3) methylprednisolone at 3 mg/kg/day (days 1–7), followed by tapering to 2 mg/kg/day (days 8–14), 1 mg/kg/day (days 15–21) and 0.5 mg/kg/day (day 22 to the time at sacrifice); (4) intravenous injection of cyclophosphamide (20 mg/kg/day) at days 0, 2, 5, and 7; (5) ganciclovir (2.5 mg/kg/day intramuscular injection (i.m.)) was also administrated to avoid viral infection in the immunocompromised host.

DNA extraction and quantification of human-derived cells

Total DNA of WHHL rabbit liver, which was obtained at the time just after hADMPC transplantation, and 2, 4, 8, and 12 weeks after transplantation, were isolated using a NucleoSpin Tissue kit (Macherey-Nagel) according to the manufacturer's instructions. hADMPCs and rabbit hepatocytes were mixed at the ratios of 100:0 (100%), 10:90 (10%), 1:99 (1%), 0.1:99.9 (0.1%), 0.01:99.99 (0.01%), and 0.001:99.999 (0.001%), and DNA was isolated. Seven hundred nanograms of each samples of extracted DNA was quantified by real-time polymerase chain reaction (PCR) using the ABI Prism 7900 Sequence Detection System (Applied Biosystems), primers for the 82 bp *Alu* amplicon (forward, 5′-GTCAGGAGATCGA GACCATCCC; reverse, 5′-CCACTACGCCCGGCTAATTT), and SYBR Green (TOYOBO) dye using a previously published protocol.[21,22] Reactions were performed in quadruplicate and the *Alu* levels were calculated by the standard curve.

Assay for lipid profiling

Serum samples were obtained from nonfasting rabbits before and after transplantation. Serum total cholesterol was measured in each sample using assay kits from Wako Pure Chemical Industries. Serum lipoproteins were analyzed by an on-line dual enzymatic method for simultaneous quantification of cholesterol and triglycerides by high-performance

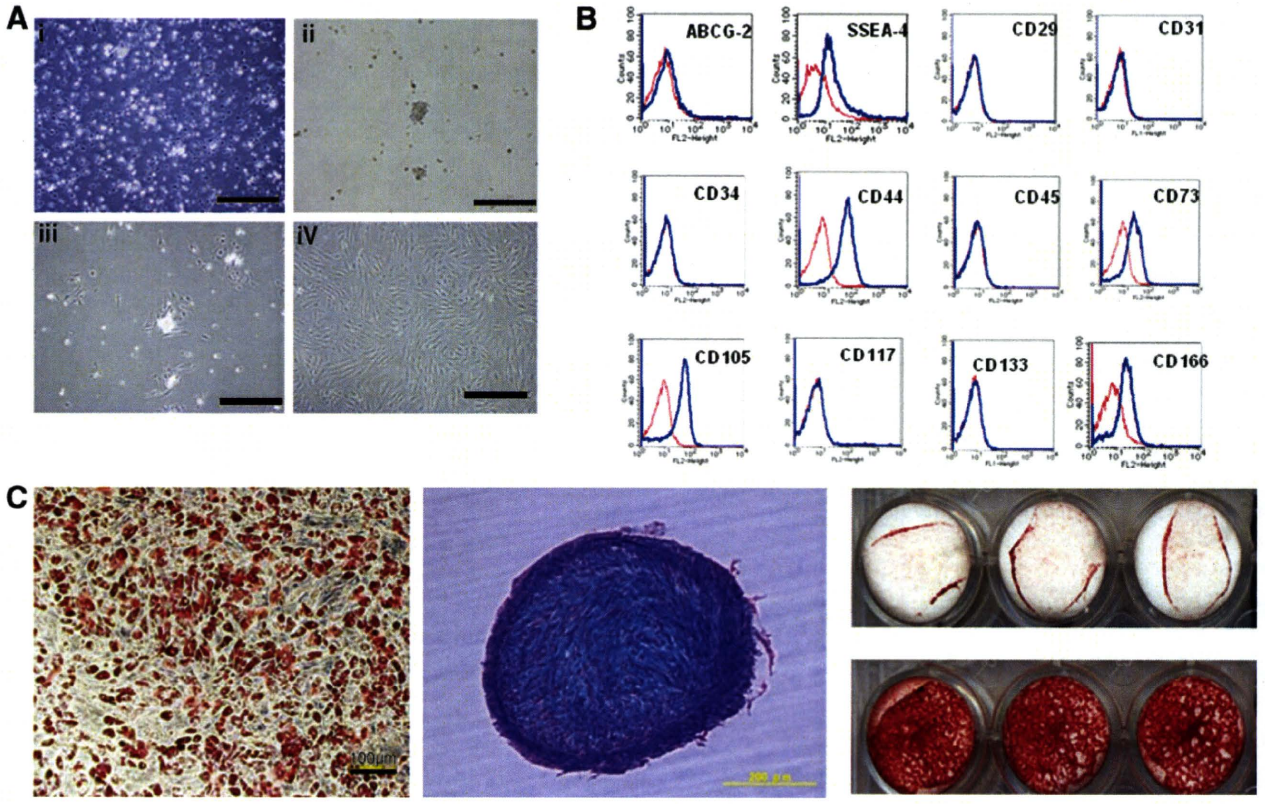

FIG. 1. **(A)** Morphological characters of human adipose tissue-derived multilineage progenitor cells (hADMPCs). The cells obtained from adipose tissue were seeded and incubated for 24 h **(i)**. After incubation, the adherent cells were treated with ethylenediaminetetraacetic acid solution, and the resulting suspended cells were replated at a density of 10,000 cells/cm^2 on human fibronectin-coated dishes (BD BioCoat) **(ii, iii)**. Within two to three passages after the initial plating of the primary culture, hADMPCs appeared as a monolayer of large flat cells (25–30 μm in diameter). As the cells approached confluence, they assumed a more spindle-shaped, fibroblastic morphology **(iv)**. i) Bar = 499 μm, ii) bar = 201 μm, iii) bar = 502 μm and iv) bar = 202 μm. **(B)** Cell surface markers expressed on hADMPCs. The cells were negative for markers of the hematopoietic lineage (CD45) and of hematopoietic stem cells, ABCG-2, CD34, and CD133. They were also negative for CD31, an endothelial cell-associated marker, and the surface antigen c-Kit (CD117). However, they stained positively for a number of surface markers characteristic of mesenchymal and/or neural stem cells, but not embryonic stem (ES) cells, including CD29, CD44 (hyaluronan receptor), CD73, CD105 (endoglin), and CD166. hADMPCs also were positive for stage-specific embryonic antigen (SSEA)-4. **(C)** Adipocytic, chondrocytic, and osteocytic differentiation potentials of hADMPCs. Adipocytic differentiation potential of hADMPCs was confirmed by Oil Red O staining (the left panel) (bar = 100 μm). Chondrocytic differentiation potential of hADMPCs was estimated by extracellular matrices with Alcian Blue staining (the middle panel). Osteogenic differentiation potential of hADMPCs was confirmed by Alizarin red S staining for mineralized nodules (the right panel).

liquid chromatography at Skylight Biotech, according to the procedure as described.[23]

Immunohistochemical staining of WHHL rabbit liver sections

The WHHL livers were harvested and fixed immediately with 10% formalin. They were placed into optimal cutting temperature compound (Sakura Finetechnical Co.), frozen immediately, and then sectioned at 7 μm thickness. The sections were then incubated with blocking solution (Blocking one; Nacalai Tesque) for 1 h. The samples were incubated with rabbit anti-human-specific albumin antibody (MBL), rabbit anti-human-specific alpha 1 anti-trypsin antibody, and rabbit anti-LDL receptor antibody, followed by Alexa Fluor 488-labeled goat anti-rabbit IgG (Molecular Probes). To show the colocalization of human CD90 and albumin, the samples were incubated with the rabbit anti-human CD90 monoclonal antibody (Epitomics, Inc.) and then with Alexa Fluor 488-labeled goat anti-rabbit IgG (Molecular Probes), and washed extensively. Then, the specimens were incubated with rabbit anti-human-specific albumin antibody (MBL), followed by Alexa Fluor 546-labeled goat anti-rabbit IgG (Molecular Probes). The treated sample was examined with a BioZero laser scanning microscope (Keyence).

PCR analysis of WHHL rabbit liver for human liver-specific genes

Total RNAs of WHHL rabbit liver, hADMPCs, and human hepatocytes were isolated using an RNAeasy kit (Qiagen). After treatment with DNase, the cDNA was synthesized using Superscript III RNase H-minus Reverse Transcriptase (Invitrogen). Real-time PCR was performed using the ABI Prism 7900 Sequence Detection System (Applied Biosystems). About 20× Assays-on-Demand™ Gene Expression Assay Mix for human alpha-1-antitrypsin (Hs01097800_m1), human albumin (Hs00609411_m1), human factor 9, human GATA-binding

protein 4 (GATA4) (Hs00171403_m1), human hepatocyte nuclear factor 3 beta (Hs00232764_m1), human LDL receptor (Hs00181192_m1), and human glyceraldehyde-3-phosphate dehydrogenase (Hs99999905_m1) were obtained from Applied Biosystems. It was confirmed that human detectors and rabbit detectors do not cross-react with the other species. TaqMan® Universal PCR Master Mix, No AmpErase® UNG (2×), was also purchased from Applied Biosystems. Reactions were performed in quadruplicate and the mRNA levels were normalized relative to human glyceraldehyde-3-phosphate dehy-

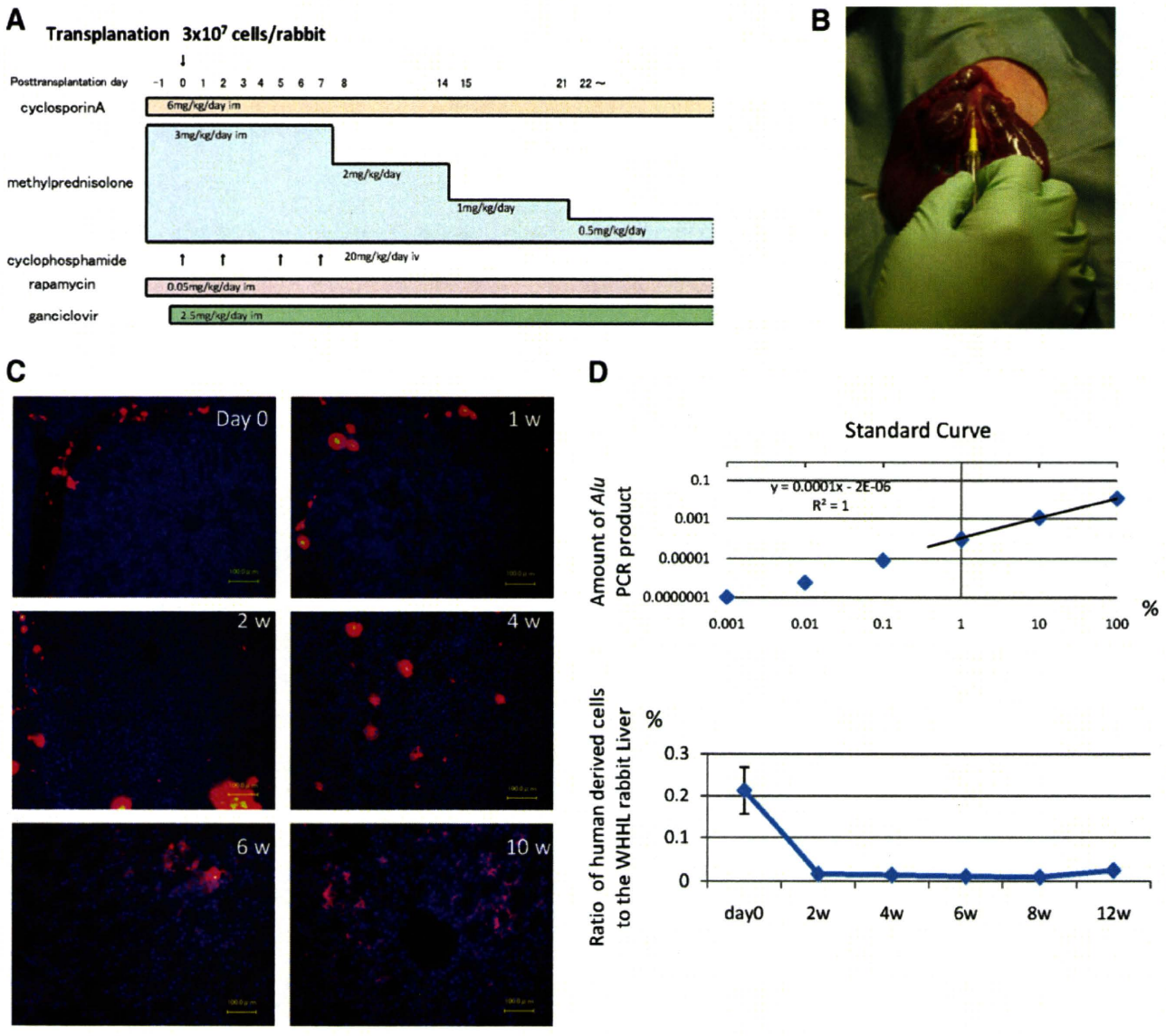

FIG. 2. **(A)** Immunosuppression regimen. Cyclosporin A (6 mg/kg/day) and rapamycin (0.05 mg/kg/day) were administered intramuscularly daily from the day before surgery to sacrifice. Methylprednisolone was administered at 3 mg/kg/day (days 1–7), 2 mg/kg/day (days 8–14), 1 mg/kg/day (days 15–21), and 0.5 mg/kg/day (day 22 to sacrifice). Cyclophosphamide (20 mg/kg/day) was injected intravenously at days 0, 2, 5, and 7. Ganciclovir (2.5 mg/kg/day) was also injected intramuscularly to avoid viral infection in the immunocompromised host. **(B)** Surgical procedure. Watanabe heritable hyperlipidemic (WHHL) rabbits were anesthetized with pentobarbital. An incision was made distal and parallel to the lower end of the ribcage. The peritoneum was incised and hADMPCs, and human adipose tissue-derived fibroblastic cells (hADFCs) (3×10^7 cells/rabbit) or controls were infused into the portal vein using an 18-gauge Angiocath. **(C)** Localization of transplanted hADMPCs in the WHHL liver. At the day of and 1, 2, 4, 6, and 10 weeks after transplantation of DiI-labeled hADMPCs via the portal vein, the WHHL rabbit liver was examined histologically. DiI-fluorescent labeled-hADMPCs resided and distributed in the portal area at the day of transplantation. One to 2 weeks after transplantation, the DiI-stained hADMPCs-derived cells were localized near the portal areas. Four weeks after transplantation some of the DiI-stained cells resembled innate hepatocytes morphologically. Six and 10 weeks after transplantation, DiI-positive transplanted cells were dispersed in a centrilobular direction, resembling the mature innate hepatocytes. Bars = 100 μm. **(D)** Quantification of repopulation of the transplanted cells in the liver. The ratios of human-derived cell repopulation were examined by analyzing an *Alu* repetitive DNA sequence at the day of and 2, 4, 8, and 12 weeks after transplantation. In upper panel the standard curve was indicated, and in lower panel the ratio of repopulation of human cells was shown in time course after transplantation of hADMPCs.

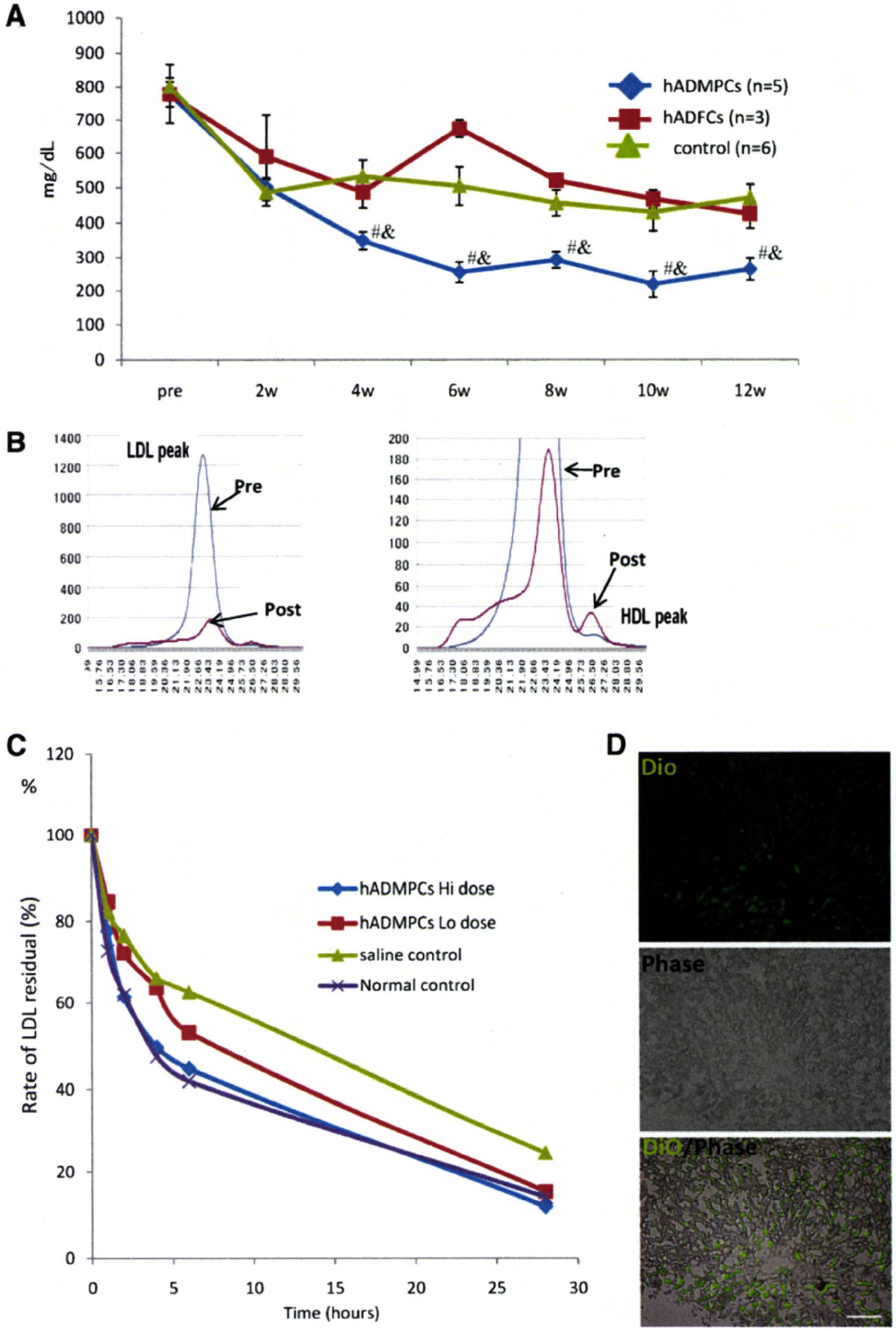

FIG. 3. **(A)** Total serum cholesterol levels. hADMPC transplantation in WHHL rabbits was followed for 12 weeks. Total serum cholesterol was measured in five rabbits that each received 3×10^7 hADMPCs, three rabbits that each received 3×10^7 hADFCs, and in six rabbits that received saline (control). Bars indicated mean ± standard error of the mean (SEM) ($^{\#}p < 0.05$; control vs. the hADMPC-transplanted WHHL rabbit; $^{\&}p < 0.05$; the hADFC-transplanted WHHL rabbit vs. the hADMPC-transplanted WHHL rabbit). **(B)** Lipoprotein profiles in a representative WHHL rabbit with hADMPC transplantation after gel filtration. Serum samples from the WHHL rabbit before and 4 weeks after transplantation were fractionated. Note the marked reduction in low-density lipoprotein (LDL) peak and appearance of high-density lipoprotein (HDL) peak. **(C)** Rate of clearance of LDL from the serum of rabbits with and without transplantation of hADMPCs. Animals were injected with ^{125}I-labeled human LDL, and the time course of clearance was monitored following trichroloacetic acid precipitation of serum at time 5 min, 1 h, 2 h, 4 h, 6 h, and 28 h. Residual ^{125}I-LDL was expressed as percentages of that at 5 min. $^{\#}p < 0.05$ (control vs. the hADMPC-transplanted WHHL rabbit [low dose]) and $^{*}p < 0.05$ (control vs. the hADMPC-transplanted WHHL rabbit [high dose]). **(D)** DiO-LDL uptake into hADMPC-derived hepatocytes in the WHHL rabbi liver. Thin-sliced recipient liver was incubated with DiO-labeled LDL in the serum-free medium for 24 h. After washing and fixation, the incubated slices were applied for fluorescent microscopy. DiO-LDL uptake cells (green) and no uptake parenchymal cells were observed in the section. Bar = 100 μm.

drogenase expression. To confirm that hADMPCs differentiated into hepatocytes *in vivo*, the cells before transplantation and human primary hepatocytes (Invitrogen, Lot number; HuP81) were applied for quantitative PCR as control.

Clearance of ^{125}I-LDL from rabbit serum

WHHL rabbits (8 weeks old) were anesthetized with pentobarbital (50 mg/kg). The peritoneum was incised and hADMPCs (high-dose; 3×10^7 cells/rabbit, $n=2$, low-dose; 5×10^6 cells/rabbit, $n=2$) suspended in 3 mL of HBSS (20°C) ($n=5$) or 3 mL of control saline ($n=2$) were infused into the portal vein via a 18-gauge Angiocath (BD). The rabbits were immunosuppressed using the protocol illustrated in Figure 1A. Eight weeks later, the animals were tested by the LDL turnover assay. ^{125}I human LDL (BT-913R, Lot No. 9130709; Biomedical Technologies Inc.) was delivered via the marginal ear vein of the WHHL rabbits and normal control

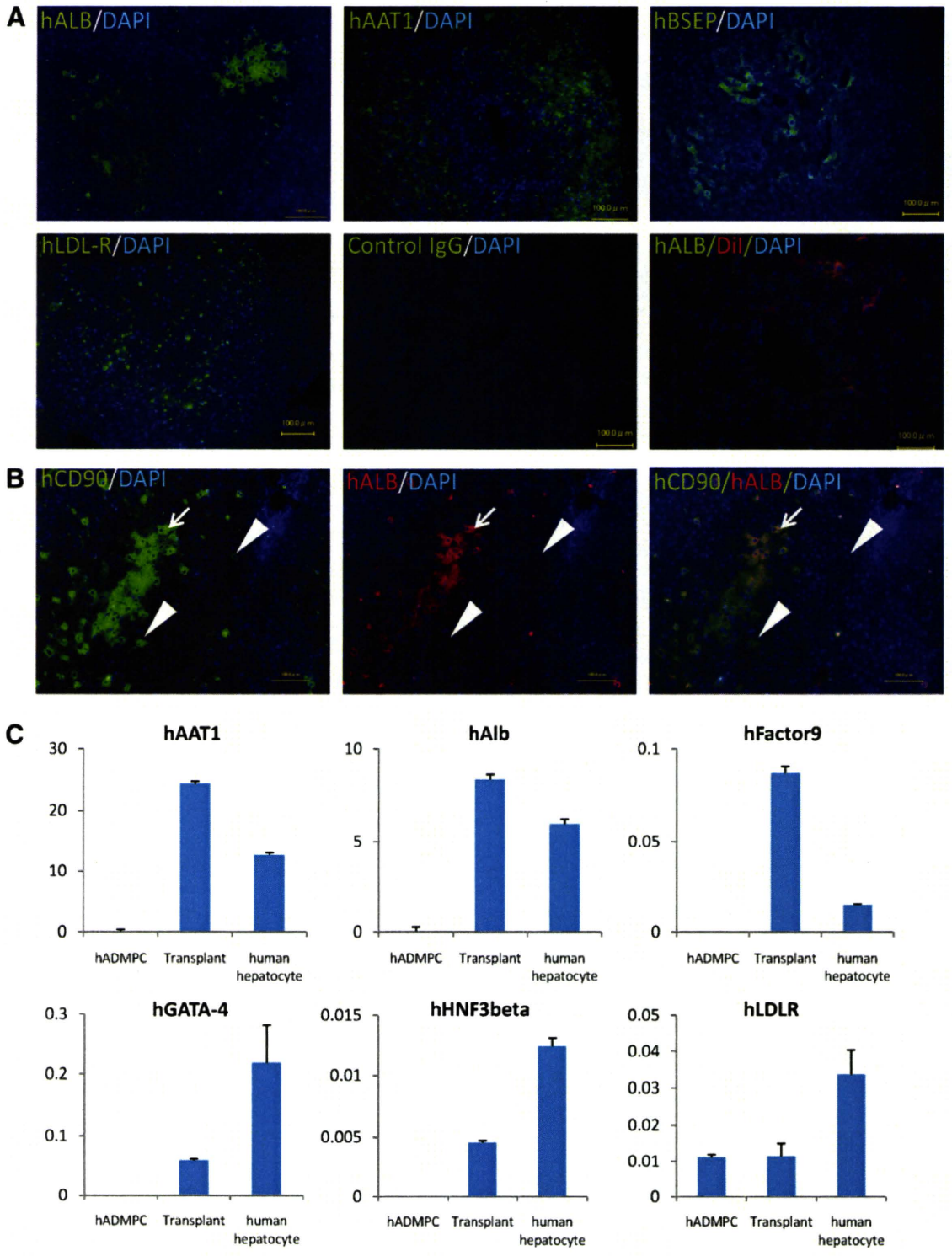

rabbits in physiological saline containing 2 mg/mL bovine serum albumin. Blood was collected from the opposite ear after injection at 5 min, 1 h, 2 h, 4 h, 6 h, and 28 h. ^{125}I-labeled apolipoprotein B-containing LDL was precipitated with 20% of trichloroacetic acid (Wako Pure Chemical Industries) (serum; 320 μL, 100% w/v trichloroacetic acid (TCA) 80 μL), and then the precipitants were applied for counting.

Uptake of DiO-labeled LDL by transplants ex vivo

Human LDL (1.019–1.063 g/mL) was isolated by sequential ultracentrifugation from normolipidemic donors as previously described,[24] dialyzed against saline-EDTA, and then sterilized by filtration through a 0.2 μm filter. Lipoproteins were labeled with 3,3′-dioctadecyloxacarbocyanine perchlorate (DiO; Sigma) by incubating the LDL in 0.5% bovine serum albumin/PBS with 100 mL DiO in dimethyl sulfoxide (3 mg/mL) for 8 h at 37°C. The lipoproteins were obtained by sequential ultra centrifugation (1.019–1.063 g/mL) as described,[14] and then dialyzed against PBS and filtered before use. To evaluate the uptake of DiO-LDL by transplants *ex vivo*, thin-sliced WHHL rabbit liver tissue were incubated with serum-free Dulbecco's modified Eagle's medium containing 10 μg/mL DiO-LDL for 24 h at 37°C. Finally, the incubated slices were rinsed, fixed with 10% formalin, sectioned into 5 μm thickness, and mounted with Perma-Flour (Japan Tanner Corporation). The slides were examined using a BioZero laser scanning microscope (Kyence).

Statistical analysis

Values were expressed as mean ± standard error of the mean. Differences between mean values of treated and untreated groups were evaluated using the Student's *t*-test. A p-value < 0.05 was considered statistically significant. All statistical analyses were performed using the SPSS Statistics 17.0 package (SPSS Inc.).

Results

Characteristics of hADMPCs

The cells obtained from adipose tissue were seeded and incubated for 24 h (Fig. 1Ai). After incubation, the adherent cells were treated with EDTA solution, and the resulting suspended cells were replated at a density of 10,000 cells/cm^2 on human fibronectin-coated dishes (BD BioCoat) (Fig. 1Aii and 1Aiii). Within two to three passages after the initial plating of the primary culture, hADMPCs appeared as a monolayer of large flat cells (25–30 μm in diameter). As the cells approached confluence, they assumed a more spindle-shaped, fibroblastic morphology (Fig. 1Aiv). After passaging five to six times, the hADMPCs were applied for transplantation. We used flow cytometry to assess markers expressed by hADMPCs (Fig. 1B). The cells were negative for markers of the hematopoietic lineage (CD45) and of hematopoietic stem cells, ABCG-2, CD34, and CD133. They were also negative for CD31, an endothelial cell-associated marker and the surface antigen c-Kit (CD117). However, they stained positively for a number of surface markers characteristic of mesenchymal and/or neural stem cells, but not embryonic stem cells, including CD29, CD44 (hyaluronan receptor), CD73, CD105 (endoglin), and CD166. hADMPCs also were positive for stage-specific embryonic antigen-4. Next, adipogenic, osteogenic, and chondrogenic differentiation potential of hADMPCs were examined (Fig. 1C). Adipogenic differentiation was induced by culture with differentiation medium containing 1-methyl-3-isobutylxanthine (a peroxisome proliferator-activated receptor γ agonist), dexamethasone, and insulin. Induction was confirmed by the accumulation of intracellular lipid droplets that were stained with Oil Red O. After 7-day induction for osteogenesis, hADMPCs were stained with Alizarin red S for mineralized nodules. hADMPCs showed intense Alcian Blue staining, indicating chondrogenic induction capability of hADMPCs.

Serum cholesterol in WHHL rabbit with transplants

hADMPCs were separated from human subcutaneous adipose tissues, cultured for five to seven passages, and applied for transplantation into WHHL rabbits. WHHL rabbits received immunosuppressants and an antiviral agent as illustrated in Figure 2A, and then were transplanted 3×10^7 hADMPCs by portal vein infusion (Fig. 2B). At the day of and 1, 2, 4, 6, and 10 weeks after transplantation of hADMPCs via the portal vein, we examined whether the cells reside or not in the liver after transplantation. Typical

FIG. 4. **(A)** Immunohistochemical identification of human hepatocytic marker cells in liver sections of WHHL rabbits after hADMPC transplantation. Twelve weeks after hADMPC transplantation, human albumin-, human alpha-1-antitrypsin-, human bile salt export pump (BSEP)-, and LDL-receptor-positive cells were dispersed within the perivenous regions of the liver parenchyma, where they made contact with and integrated among the host cells with cell–cell interactions between hADMPC-derived cells and diseased hepatocytes pair. Ten weeks after transplantation of DiI-stained hADMPCs, copresence of human albumin (green) and pretreated DiI-fluorescence (red) on the same cells was observed. Bar = 100 μm. **(B)** Differentiation of transplanted hADMPCs into hepatocyte-like cells. Twelve weeks after transplantation, almost but not all human CD90-positive cells expressed human albumin, indicating that major population of transplanted hADMPCs could differentiate into hepatocyte-like cells (left panel: human CD90; middle panel: human albumin; right panel: merge). Arrows indicate human CD90 and human albumin double-positive cells; arrowheads indicate human CD90-positive but human albumin-negative cells. **(C)** Human hepatic gene expression in WHHL rabbit liver after hADMPC transplantation. RNA was prepared from the WHHL rabbit liver 12 weeks after hADMPC transplantation. We used the following hepatic markers: human alpha-1-antitrypsin, human albumin, human factor IX, human GATA-binding protein 4 (GATA-4), human hepatocyte nuclear factor 3 (HNF-3) beta, and human LDL-receptor. Their expression levels were examined by quantitative real time-polymerase chain reaction (RT-PCR) using Assays-on-Demand Gene Expression Assay Mix. The livers of WHHL rabbits that received saline ($n = 3$) were negative for human hepatic genes. The mRNA levels were normalized based on human glyceraldehyde-3-phosphate dehydrogenase expression as housekeeping gene and data are mean ± SEM of triplicate experiments. The livers of WHHL rabbits that received hADMPC transplantation ($n = 3$) were positive for human hepatic genes, and their expression levels were similar to those of human primary hepatocytes but not hADMPCs *per se*. Data are mean ± SEM.

distribution patterns of transplanted hADMPCs were followed in Figure 2C. DiI-fluorescent labeled-hADMPCs resided and distributed in the portal area at the day of transplantation. Six and 10 weeks after transplantation, DiI-positive transplanted cells migrated into centrilobular direction. Next, to demonstrate certain percentage of repopulation of the transplanted cells in the liver, the ratios of human-derived cell repopulation were examined by analyzing a repetitive DNA sequence at the day of and 2, 4, 6, and 12 weeks after transplantation (Fig. 2D). To indicate standard curve, we mixed the indicated percentage of hADMPCs with rabbit hepatocytes and plotted the obtained the amount of *Alu* PCR products, and estimated the amount of repopulation of the transplanted cells in the liver. At the day of transplantation, the ratio of hADMPCs to whole WHHL rabbit liver cells was $0.21\% \pm 0.056\%$ (mean $\pm$ standard error of the mean) and the ratio decreased to $0.016\% \pm 0.002\%$, $0.011\% \pm 0.001\%$, and $0.009\% \pm 0.0001\%$ after 2, 4, and 8 weeks of transplantation, respectively. After 12 weeks of transplantation, the ratio was increased to $0.024\% \pm 0.00005\%$ as indicated (Fig. 2D).

To reveal the effects of hADMPC transplantation onto the lipid profiles of the WHHL rabbit, serum cholesterol levels were monitored over 12 weeks (Fig. 3A). Significant reductions in total serum cholesterol were observed within 4 weeks of the transplantation, and the reductions were maintained for the entire period. The reduction in serum cholesterol in the animals that received hADMPC transplantation was significantly greater than that of the control group. To determine the effects of hADMPC transplantation on the fractions of high-density lipoprotein and LDL in recipient animals, fractionation by fast protein liquid chromatography was performed (Fig. 3B). Transplantation of hADMPCs resulted in marked reduction of the peak LDL-cholesterol and increment of high-density lipoprotein cholesterol fraction (right panel).

Next, clearance experiments were performed with human LDL to confirm that the transplanted hADMPCs contributed the fall in serum cholesterol through uptake of LDL via LDL receptors. The rate of LDL clearance was significantly higher in the WHHL rabbits with transplanted hADMPCs than WHHL rabbits without transplanted hADMPCs (Fig. 3C). Rabbits with hADMPC transplants showed $\sim$2.4-fold (high-dose; 3×10^7 cells/rabbit) and 1.4-fold (low-dose; 5×10^6 cells/rabbit) increase in the rate of LDL cholesterol clearance.

To evaluate the uptake of DiO-LDL by transplants *ex vivo*, thin-sliced WHHL rabbit liver was incubated with DiO-labeled LDL for 24 h and the uptake was examined as clearance experiment (Fig. 3D). DiO-LDL was uptaken by some but not all of the cells in the WHHL rabbit liver transplanted with hADMPCs. The DiO-LDL-uptaking cells were seen dispersed, contacted, and integrated among the nonuptaking parenchymal cells, suggesting that hADMPCs differentiated into hepatocytes *in vivo*, lowered of serum cholesterol via LDL uptake.

hADMPCs reside, survive, and differentiate into hepatocytes in vivo

After establishment of the graft as indicated by long-term lowering of serum cholesterol, human-specific hepatocytic proteins, such as albumin, alpha-1-antitrypsin, bile salt export pump, and LDL-receptor, positive cells were identified dispersed within perivenous regions of the liver parenchyma, where they have contacted and integrated among the host cells (Fig. 4A), with cell–cell interactions conserved between hADMPC-derived hepatocytes and diseased hepatocytes pair. Ten weeks after transplantation of DiI-prestained hADMPCs, copresence of human albumin (green) and pretreated DiI-fluorescence (red) on the same cells was observed (Fig. 4A), indicating the transplanted hADMPCs might differentiate into hepatocyte-like cells. To confirm transplanted hADMPCs might differentiate into hepatocyte-like cells and to reveal the efficacy of differentiation, the colocalization of human CD90 and human albumin was examined. As shown in Figure 4B, almost but not all human CD90-positive cells expressed human albumin, indicating that about 80% or more of transplanted hADMPCs could differentiated into human albumin-positive hepatocyte-like cells 12 weeks after transplantation. Next, to confirm the differentiation of hADMPCs into hepatocytes *in vivo*, expression of hepatocyte markers was analyzed by quantitative RT-PCR. The WHHL rabbit liver that was transplanted with hADMPCs expressed higher levels of human-specific alpha-1-antitrypsin, albumin, and coagulation factor IX than hADMPCs (Fig. 4C). The expression levels of human GATA-4, human hepatocyte nuclear factor 3 beta, and LDL-receptor were also higher in the WHHL rabbit liver than hADMPCs (Fig. 4C). These results indicate that hADMPCs differentiate into mature hepatocytes *in vivo*.

Discussion

We have used the WHHL rabbit to study the ability of hADMPC-derived hepatocytes to lower serum cholesterol in an animal model of FH. Our results have shown that hADMPCs transplanted into the rabbit liver differentiate into hepatocytes *in vivo* and effectively clear LDL from the circulation.

The reductions in cholesterol brought about by the engrafted hADMPC-derived hepatocytes suggest that human LDL receptors can act as replacement for the mutant LDL receptors in the WHHL rabbit. This capacity of hADMPC-derive hepatocytes is not unexpected, as the liver is the most important site of LDL uptake, accounting for >50% of total removal from the circulation, and the liver is only organ capable of converting cholesterol to bile for excretion. The substantial decrease in serum cholesterol achieved suggests that the hADMPC-derived hepatocytes both internalize LDL and metabolize the cholesterol to bile for excretion. The correlation between cholesterol and coronary heart disease has been well documented, and decreases in serum cholesterol of the magnitude that we have demonstrated would be expected to decrease morbidity and mortality in the patients with severe FH.[25]

The appearance of the hADMPC-derived hepatocytes as revealed by immunohistochemistry and RT-PCR indicated that the hADMPCs differentiated into hepatocytes and integrated into the liver parenchyma. The perivenous migration of the differentiated hepatocytes derived from hADMPCs along the portal-venous axis and suggests that hADMPCs recognize conserved signals on host cells and matrix. There are some reports describing the hepatogenic differentiation potential of hADMPCs.[15,16] These studies

described that hepatocytes differentiated from hADMPCs *ex vivo* engrafted in the liver and functioned, and that the hADMPCs could be resided and changed their characters into hepatocyte-like cells only in the chemically damaged liver. These reports, revealing that hADMPCs have capabilities to differentiate into hepatocytes, hinted us that hADMPCs might differentiate into hepatocytes in liver. Hepatogenic signals from the microenvironment such as cell-to-cell connections or intermediates are probably important factors that dictate the type of functional hepatocytes in hepatic differentiation.[26] We are currently investigating the mechanism for the differentiation hADMPCs into hepatocytes.

The choice of cell source is critical for realizing success in cellular therapy. Liposuction surgeries yield a massive amount of lipoaspirate adipose tissue from 100 mL to >3 L as cell sources.[27] A major advantage of hADMPCs is their availability in safe and easy with few ethical issues, as compared with the shortage of human livers for orthotopic transplantation, which has been shown to be effective for the treatment of FH.[25] Our serum cholesterol reduction studies and *in vitro* studies demonstrated that human LDL binds to the hADMPC-derived hepatocytes receptor, indicating that this therapy will be useful in humans. Previous attempts to study the efficacy of hepatocyte transplantation in the WHHL rabbit model have employed allogenic hepatocytes, xenogenic hepatocytes, or hepatocytes transduced *ex vivo* with a recombinant retrovirus containing the LDL receptor cDNA.[6–13] The lowering effects of hepatocyte transplantation on serum cholesterol have been reported, but there was some problems. First, hepatocytes could not be expanded *ex vivo* with functional potentials; second, the cell viability reduced after cryopreservation; third, the many injected hepatocytes are supposed to be cleared by the reticuloendothelial system or lose viability during early phase. The rate of LDL clearance was returned to normal in LDL receptor knockout mice by introduction of an adenoviral construct containing an LDL receptor cDNA, and similar approaches have lowered serum cholesterol levels in the WHHL rabbit.[10,12,13] However, sustained expression of the LDL receptor from viral vectors can be difficult to achieve.[11,13] Moreover, hepatocytes derived from hADMPCs have the advantage that the LDL receptor is expressed from an endogenous gene with intact regulatory sequences. Such control of LDL receptor levels would not be expected after treatment of hypercholesterolemia with LDL receptor cDNA construct that lack the regulatory regions of the gene.[28]

Our experiments have shown that the hADMPCs expressed hepatocyte markers after transplantation *in vivo* and the integrated cells into parenchyma provide functional LDL receptors, indicating that they differentiated into hepatocytes and might lower serum cholesterol in the WHHL rabbit. These results suggested that hADMPC transplantation via portal vein could correct the metabolic defects of FH patients and that hADMPC-derived hepatocytes could function as supplier with plasma proteins derived from liver, giving us an idea that hADMPC-transplantation might be a novel cell therapy for hemophilia, alpha-1 antitrypsin deficiency, mucolipidosis, and other diseases caused by genetic defects for liver function. In near future, the therapy will be a novel therapy for kinds of inherited liver diseases.

Acknowledgments

This study was supported in part by the Program for Promotion of Fundamental Studies in Health Sciences of the National Institute of Biomedical Innovation (NIBIO), RIKEN Program for Drug Discovery and Medical Technology Platforms, and Kobe Translational Research Cluster, the Knowledge Cluster Initiative, Ministry of Education, Culture, Sports, Science and Technology (MEXT).

Disclosure Statement

All of the authors stated no conflict of interest.

References

1. Brown, M.S., and Goldstein, J.L. A receptor-mediated pathway for cholesterol homeostasis. Science **232,** 34, 1986.
2. Havel, R.J., Yamada, N., and Shames, D.M. Watanabe heritable hyperlipidemic rabbit. Animal model for familial hypercholesterolemia. Arteriosclerosis **9(1 Suppl),** I33, 1989.
3. Yamamoto, T., Bishop, R.W., Brown, M.S., Goldstein, J.L., and Russell, D.W. Deletion in cysteine-rich region of LDL receptor impedes transport to cell surface in WHHL rabbit. Science **32,** 1230, 1986.
4. Bujo, H., Takahashi, K., Saito, Y., Maruyama, T., Yamashita, S., Matsuzawa, Y., Ishibashi, S., Shionoiri, F., Yamada, N., and Kita, T. Clinical features of familial hypercholesterolemia in Japan in a database from 1996–1998 by the research committee of the ministry of health, labour and welfare of Japan. J Atheroscler Thromb **11,** 146, 2004.
5. Yamashita, S., Hbujo, H., Arai, H., Harada-Shiba, M., Matsui, S., Fukushima, M., Saito, Y., Kita, T., and Matsuzawa, Y. Long-term probucol treatment prevents secondary cardiovascular events: a cohort study of patients with heterozygous familial hypercholesterolemia in Japan. J Atheroscler Thromb **15,** 292, 2008.
6. Gunsalus, J.R., Brady, D.A., Coulter, S.M., Gray, B.M., and Edge, A.S. Reduction of serum cholesterol in Watanabe rabbits by xenogeneic hepatocellular transplantation. Nat Med **3,** 48, 1997.
7. Tejera, M.L., Cienfuegos, J.A., Maganto, P., Pardo, F., Santamaria, L., Codesal, J., De Andres, S., Hernandez, J.L., and Castillo-Olivares, J.L. Reduction of cholesterol levels following liver cell grafting in hyperlipidemic (WHHL) rabbits. Transplant Proc **24,** 160, 1992.
8. Wang, J., Pollak, R., and Bartholomew, A. Sustained reduction of serum cholesterol levels following allo-transplantation of parenchymal hepatocytes in Watanabe rabbits. Transplant Proc **23,** 894, 1991.
9. Wiederkehr, J.C., Kondos, G.T., and Pollak, R. Hepatocyte transplantation for the low-density lipoprotein receptor-deficient state. A study in the Watanabe rabbit. Transplantation **50,** 466, 1990.
10. Chowdhury, J.R., Grossman, M., Gupta, S., Chowdhury, N.R., Baker, J.R., Jr., and Wilson, J.M. Long-term improvement of hypercholesterolemia after *ex vivo* gene therapy in LDLR-deficient rabbits. Science **254,** 1802, 1991.
11. Ishibashi, S., Brown, M.S., Goldstein, J.L., Gerard, R.D., Hammer, R.E., and Herz, J. Hypercholesterolemia in low density lipoprotein receptor knockout mice and its reversal by adenovirus-mediated gene delivery. J Clin Invest **92,** 883, 1993.
12. Kozarsky, K.F., McKinley, D.R., Austin, L.L., Raper, S.E., Stratford-Perricaudet, L.D., and Wilson, J.M. *In vivo* correction

of low density lipoprotein receptor deficiency in the Watanabe heritable hyperlipidemic rabbit with recombinant adenoviruses. J Biol Chem **269,** 13695, 1994.
13. Wilson, J.M., Chowdhury, N.R., Grossman, M., Wajsman, R., Epstein, A., Mulligan, R.C., and Chowdhury, J.R. Temporary amelioration of hyperlipidemia in low density lipoprotein receptor-deficient rabbits transplanted with genetically modified hepatocytes. Proc Natl Acad Sci U S A **87,** 8437, 1990.
14. Okura, H., Komoda, H., Saga, A., Kakuta-Yamamoto, A., Hamada, Y., Fumimoto, Y., Lee, C.M., Ichinose, A., Sawa, Y., and Matsuyama, A. Properties of hepatocyte-like cell clusters from human adipose tissue-derived mesenchymal stem cells. Tissue Eng Part C Methods **16,** 761, 2010.
15. Banas, A., Teratani, T., Yamamoto, Y., Tokuhara, M., Takeshita, F., Quinn, G., Okochi, H., and Ochiya, T. Adipose tissue-derived mesenchymal stem cells as a source of human hepatocytes. Hepatology **46,** 219, 2007.
16. Seo, M.J., Suh, S.Y., Bae, Y.C., and Jung, J.S. Differentiation of human adipose stromal cells into hepatic lineage *in vitro* and *in vivo*. Biochem Biophys Res Commun **328,** 258, 2005.
17. Komoda, H., Okura, H., Lee, C.M., Sougawa, N., Iwayama, T., Hashikawa, T., Saga, A., Yamamoto, A., Ichinose, A., Murakami, S., Sawa, Y., and Matsuyama, A. Reduction of N-glycolylneuraminic acid xenoantigen on human adipose tissue-derived stromal cells/mesenchymal stem cells leads to safer and more useful cell sources for various stem cell therapies. Tissue Eng Part A **16,** 1143, 2010.
18. Okura, H., Matsuyama, A., Lee, C.M., Saga, A., Kakuta-Yamamoto, A., Nagao, A., Sougawa, N., Sekiya, N., Takekita, K., Shudo, Y., Miyagawa, S., Komoda, H., Okano, T., and Sawa, Y. Cardiomyoblast-like cells differentiated from human adipose tissue-derived mesenchymal stem cells improve left ventricular dysfunction and survival in a rat myocardial infarction model. Tissue Eng Part C Methods **16,** 417, 2010.
19. Bjorntorp, P., Karlsson, M., Pertoft, H., Pettersson, P., Sjostrom, L., and Smith, U. Isolation and characterization of cells from rat adipose tissue developing into adipocytes. J Lipid Res **19,** 316, 1978.
20. Zuk, P.A., Zhu, M., Ashjian, P., De Ugarte, D.A., Huang, J.I., Mizuno, H., Alfonso, Z.C., Fraser, J.K., Benhaim, P., and Hedrick, M.H. Human adipose tissue is a source of multipotent stem cells. Mol Biol Cell **13,** 4279, 2002.
21. Nicklas, J.A., and Buel, E. Development of an Alu-based, real-time PCR method for quantitation of human DNA in forensic samples. J Forensic Sci **48,** 936, 2003.
22. Opel, K.L., Fleishaker, E.L., Nicklas, J.A., Buel, E., and McCord, B.R. Evaluation and quantification of nuclear DNA from human telogen hairs. J Forensic Sci **53,** 853, 2008.
23. Okazaki, M., Usui, S., Ishigami, M., Sakai, N., Nakamura, T., Matsuzawa, Y., and Yamashita, S. Identification of unique lipoprotein subclasses for visceral obesity by component analysis of cholesterol profile in high-performance liquid chromatography. Arterioscler Thromb Vasc Biol **25,** 578, 2005.
24. Bier, D.M., and Havel, R.J. Activation of lipoprotein lipase by lipoprotein fractions of human serum. J Lipid Res **11,** 565, 1970.
25. Steinberg, D., and Witztum, J.L. Current concepts. Lipoproteins and atherogenesis. Current concepts. JAMA **264,** 3047, 1990.
26. Hughes, R.D., Mitry, R.R., and Dhawan, A. Hepatocyte transplantation for metabolic liver disease: UK experience. J R Soc Med **98,** 341, 2005.
27. Gimble, J.M., Katz, A.J., and Bunnell, B.A. Adipose-derived stem cells for regenerative medicine. Circ Res **100,** 1249, 2007.
28. Bilheimer, D.W., Goldstein, J.L., Grundy, S.M., Starzl, T.E., and Brown, M.S. Liver transplantation to provide low-density-lipoprotein receptors and lower plasma cholesterol in a child with homozygous familial hypercholesterolemia. N Engl J Med **311,** 1658, 1984.

Address correspondence to:
Akifumi Matsuyama, M.D., Ph.D.
Department of Somatic Stem Cell Therapy and Health Policy
Foundation for Biomedical Research and Innovation
TRI305, 1-5-4 Minatojima-minamimachi, Chuo-ku
Kobe 650-0047
Japan

E-mail: akifumi-matsuyama@umin.ac.jp

Received: March 7, 2010
Accepted: August 9, 2010
Online Publication Date: September 21, 2010

GENE DELIVERY

Journal of Controlled Release 148 (2010) 212–218

Contents lists available at ScienceDirect

Journal of Controlled Release

journal homepage: www.elsevier.com/locate/jconrel

Adenovirus serotype 35 vector-induced innate immune responses in dendritic cells derived from wild-type and human CD46-transgenic mice: Comparison with a fiber-substituted Ad vector containing fiber proteins of Ad serotype 35

Fuminori Sakurai [a,b,1,*], Kazuko Nakashima [a,1], Tomoko Yamaguchi [a,b], Takako Ichinose [a], Kenji Kawabata [a,c], Takao Hayakawa [d], Hiroyuki Mizuguchi [a,b,*]

[a] Laboratory of Gene Transfer and Regulation, National Institute of Biomedical Innovation, Ibaraki-City, Osaka, Japan
[b] Department of Biochemistry and Molecular Biology, Graduate School of Pharmaceutical Sciences, Osaka University, Suita-City, Osaka, Japan
[c] Graduate School of Pharmaceutical Sciences, Osaka University, Suita-City, Osaka, Japan
[d] Pharmaceutical Research and Technology Institute, Kinki University, Osaka, Japan

ARTICLE INFO

Article history:
Received 18 May 2010
Accepted 19 August 2010
Available online 26 August 2010

Keywords:
Adenovirus serotype 35 vectors
Fiber-substituted Ad vectors
Innate immunity
CD46
Dendritic cells
Inflammatory cytokine

ABSTRACT

Recently, much attention has focused on replication-incompetent adenovirus (Ad) vectors containing fiber proteins derived from species B Ad serotype 35 (Ad35) (Ad5F35) and Ad vectors fully constructed from Ad35 as vaccine vectors expressing antigens. However, differences in the transduction properties, including the induction of innate immunity, of Ad5F35 and Ad35 vectors have not been properly and fully examined, partly because the transduction properties of these Ad vectors should be evaluated using nonhuman primates or human CD46-transgenic (CD46TG) mice, which ubiquitously express the primary receptor of Ad35, human CD46, in a pattern similar to that of humans. In the present study, we evaluated innate immune responses of mouse dendritic cells (mDCs) derived from bone marrow cells of wild-type (WT) and CD46TG mice following transduction with Ad serotype 5 (Ad5), fiber-substituted Ad5F35, or Ad35 vectors. Ad5F35 and Ad35 vectors mediated more efficient transduction in mDCs derived from CD46TG mice (CD46TG-mDCs) than did Ad5 vectors. Upregulation of costimulatory molecules and inflammatory cytokine induction by Ad5F35 and Ad35 vectors were significantly higher than those by Ad5 vectors in CD46TG-mDCs. However, the induction properties of the innate immune responses were different between Ad5F35 and Ad35 vectors. Ad35 vectors induced higher levels of costimulatory molecule expression and inflammatory cytokine production than did Ad5F35 vectors in CD46TG-mDCs. Furthermore, intravenous administration of Ad35 vectors in WT and CD46TG mice resulted in higher levels of serum interleukin (IL)-6 and IL-12 compared with administration of Ad5F35 vectors, which exhibited almost mock-transduced levels of these inflammatory cytokines. This study indicates that innate immune responses by Ad35 and Ad5F35 vectors are distinct even although both Ad vectors recognize human CD46 as a receptor.

© 2010 Elsevier B.V. All rights reserved.

1. Introduction

Replication-incompetent adenovirus (Ad) vectors have been considered promising for vaccine therapy application because Ad vectors are grown to high titers and show high transduction efficiencies. Furthermore, following transduction, Ad vectors induce innate immune responses, including inflammatory cytokine induction and upregulation of costimulatory molecules on immune cells, and these responses enhance antigen-specific immune responses as an adjuvant effect [1–4]. Ad vector-based vaccines have been used in preclinical and clinical trials for infectious diseases, including acquired immune deficiency syndrome (AIDS) caused by human immunodeficiency virus [5–7]. These preclinical and clinical studies mainly used conventional Ad vectors composed of Ad serotype 5 (Ad5), which belongs to species C. Ad5 vectors have several advantages for vaccine application; however, dendritic cells (DCs), which are professional antigen-presenting cells and the main targets of Ad vector-mediated transduction in vaccine therapy, do not express sufficient levels of a receptor for Ad5 (coxsackievirus and adenovirus receptor, CAR), leading to inefficient transduction with Ad5 vectors in DCs [4].

To overcome this problem, fiber-substituted Ad vectors containing fiber proteins of species B Ad were developed [8–10]. Most species B adenoviruses (Ads) bind to human CD46, which is ubiquitously

* Corresponding authors. Sakurai is to be contacted at Laboratory of Gene Transfer and Regulation, National Institute of Biomedical Innovation, 7-6-8 Asagi, Saito, Ibaraki-City, Osaka 567-0085, Japan. Tel.: +81 72 641 9815; fax: +81 72 641 9816. Mizuguchi, Department of Biochemistry and Molecular Biology, Graduate School of Pharmaceutical Sciences, Osaka University, 1-6 Yamadaoka, Suita, Osaka 565-0871, Japan. Tel./fax: +81 6 6879 8185.
E-mail addresses: sakurai@nibio.go.jp (F. Sakurai), mizuguch@phs.osaka-u.ac.jp (H. Mizuguchi).
[1] These two authors contributed equally to this work.

0168-3659/$ – see front matter © 2010 Elsevier B.V. All rights reserved.
doi:10.1016/j.jconrel.2010.08.025

expressed on almost all human cells, as an infectious receptor [11,12]. Fiber proteins play a main role in the attachment of species B Ads to human CD46, indicating that substitution with fiber protein of species B Ad enables Ad vectors to efficiently infect cells lacking CAR expression [4,8–10,13]. In addition to fiber-substituted Ad vectors, Ad vectors fully composed of species B Ad have been developed [14–16]. Species B Ad vectors can circumvent anti-Ad5 immunity [17,18], which is another drawback for conventional Ad5 vector-mediated vaccination, although fiber-substituted Ad vectors based on Ad5 cannot evade anti-Ad5 immunity [13]. Among species B Ads, Ad serotype 35 (Ad35) is the most promising as an Ad vector platform and as a source of fiber proteins, because Ad35 has high tropism for DCs [4,19] and low seroprevalence in adults [20,21]. Previous studies demonstrated that Ad5F35 and Ad35 vectors efficiently transduce DCs and activate antigen-specific immune responses [2,4,19,20,22]. Several studies of vaccine therapy using Ad5F35 or Ad35 vectors in non-human primates have been recently carried out and have shown promising results [23–27]. However, there is very little information about differences in transduction properties, including induction of innate immunity, of Ad5F35 and Ad35 vectors.

As described above, species B Ads, including Ad35, use human CD46 for virus attachment. However, the expression of rodent homologues of human CD46 is limited to the testis, and there is low homology in amino acid sequences between human and rodent CD46 [28]. Therefore, human CD46-transgenic (CD46TG) mice or nonhuman primates, which exhibit CD46 expression patterns similar to that of humans, should be utilized as model animals for evaluating Ad5F35 and Ad35 vectors. Data using nonhuman primates is highly valuable; however, sample size is often small in studies using nonhuman primates, as is natural in nonhuman primate studies. In contrast, large sample sizes of CD46TG mice with uniform genetic background are available, suggesting that CD46TG mice are suitable as model animals. CD46TG mice have often been used in studies of measles virus, *Neisseria meningitidis*, and *Streptococcus pyogenes*, which also utilize human CD46 [29–33].

In the present study, we compared innate immune responses induced by conventional Ad5, fiber-substituted Ad5F35, and Ad35 vectors using wild-type (WT) and CD46TG mice. Compared to the Ad5 vectors, the Ad5F35 and Ad35 vectors induced higher levels of costimulatory molecules and inflammatory cytokines following transduction in mDCs derived from CD46TG mice. Ad35 vector-induced innate immune responses were higher than those induced by Ad5F35 vectors. Following intravenous administration, Ad35 vectors induced higher or comparable levels of interleukin (IL)-6 and IL-12, compared with Ad5 vectors, in both WT and CD46TG mice. In contrast, almost mock-transduced levels of IL-6 and IL-12 were produced by Ad5F35 vectors.

2. Materials and methods

2.1. Preparation of bone marrow-derived mouse dendritic cells (mDCs)

Wild-type C57BL/6 mice, aged 6–7 weeks, were purchased from SLC Inc. (Hamamatsu, Japan). Homozygous human CD46TG mice were kindly provided by Dr. Masaru Okabe (Osaka University, Osaka, Japan) [34]. The method for mDC cultivation was adapted from that of Luts et al. [35] and slightly modified. Briefly, bone marrow cells flushed from the femurs and tibiae of WT and CD46TG mice were seeded at 5×10^6 cells per 100-mm bacterial grade culture dish in 10 ml of RPMI 1640 containing 10% heat-inactivated fetal bovine serum (FBS), 20 ng/ml recombinant murine granulocyte-macrophage colony-stimulating factor (GM-CSF) (Pepro Tech EC Ltd., London, UK), 50 μM 2-mercaptoethanol (2-ME), and antibiotics. On day 3, another 10 ml of culture medium was added to the dish. On day 6, 10 ml of the culture supernatant was collected and centrifuged at 1500 rpm for 5 min. The pellet was resuspended in fresh culture medium and returned to the original dish to conserve unattached cells. Eight-day-old mDCs were harvested and used as immature mDCs in subsequent experiments. Flow cytometric analysis indicated that more than 85% of the resulting cell population displayed characteristic DC surface markers.

2.2. Ad vector-mediated transduction in mDCs

All the Ad vectors used in this study were constructed by an improved *in vitro* ligation method [36–38]. Ad vectors expressing enhanced green fluorescence protein (GFP) (Ad5GFP, Ad5F35GFP, and Ad35GFP) or firefly luciferase (Ad5L, Ad5F35L, and Ad35L), were prepared as previously described [16,34,39]. The infectious-particle titer ratio was 1:31 for Ad5GFP, 1:22 for Ad5L, 1:11 for AdF35GFP, and 1:30 for Ad5F35L. The vector particle (VP) titer was determined by a spectrophotometrical method [40]. The infectious titer of Ad5 and Ad5F35 vectors was determined using an Adeno-X rapid titer kit (Clontech, Mountain View, CA). The plaque-forming unit (PFU)-particle ratio was 1:185 for Ad35GFP and 1:286 for Ad35L. The PFU titer of Ad35 vectors was determined using 293-E1B cells [34] by the method of Kanegae et al. [41]. mDCs were suspended in the culture medium and seeded in a 24-well plate at 5×10^5 cells/well. Ad vectors were added at 3000 VP/cell, and the suspension was incubated at 37 °C for 1.5 h with occasional gentle agitation. Following a 1.5 h-incubation, mDCs were washed, resuspended in a fresh medium, and incubated for 24 h. The transduction efficiencies and surface marker expression were analyzed after a 24 h-incubation, as described below.

2.3. Analysis of transduction efficiencies and costimulatory molecule expression on mDCs

To measure the transduction efficiencies of Ad vectors in mDCs, mDCs were harvested, washed, and resuspended in 1% FBS-PBS 24 h after transduction. GFP expression levels were assessed by flow cytometry on a FACScalibar flow cytometer using CellQuest software (Becton Dickson, Tokyo, Japan).

To evaluate the maturation of mDCs by Ad vector transduction, mDCs were harvested 24 h after transduction and suspended in a staining buffer (PBS containing 0.1% bovine serum albumin and 0.01% NaN_3). mDCs were then incubated for 30 min on ice with the anti-FcγRII/III monoclonal antibody (2.4 G2, BD Biosciences, San Diego, CA) to block nonspecific binding of the subsequently used antibody reagents. The following phycoerythrin (PE)-labeled antibodies were then added to mDCs: anti-mouse CD40 (1C10) (BD Biosciences), -mouse CD80 (16-10A1) (BD Biosciences), and -mouse CD86 antibodies (GL1) (eBioscience, San Diego, CA). After a 30 min-incubation on ice, mDCs were washed with staining buffer and subjected to flow cytometric analysis as described above. mDCs were treated with lipopolysaccharide (LPS) (Sigma-Aldrich, St.Louis, MO) at 1 μg/ml for 24 h as a positive control for phenotypical DC maturation.

2.4. In vitro induction of inflammatory cytokines and interferon (IFN)-β following Ad vector transduction in mDCs

mDCs were transduced with Ad vectors at 3000 VP/cell as described above. The cell culture supernatants were collected following a 24 h-incubation, and the concentrations of inflammatory cytokines (IL-6, IL-12, tumor necrosis factor (TNF)-α) and IFN-β in the supernatants were measured by ELISA kit (IL-6 and IL-12; R&D system, Minneapolis, MN, TNF-α; PeproTech, London, UK, IFN-β; PBL Biomedical Laboratories, Piscataway, NJ).

2.5. In vivo induction of inflammatory cytokines following intravenous administration of Ad vectors

Ad vectors expressing firefly luciferase were intravenously administered to WT and CD46TG mice at a dose of 1.5×10^{10} VP/mouse. Six hours following administration, blood samples were collected via retro-orbital bleeding, and subjected to measurement of IL-6 and IL-12 concentration by ELISA kit.

2.6. Ad vector accumulation in the spleen following intravenous administration

Ad vectors were intravenously administered to WT and CD46TG mice at a dose of 1.5×10^{10} VP/mouse. Three hours after Ad vector injection, the spleens were harvested, and total DNA including the Ad vector genome was isolated from the spleens. The copy number of the Ad vector genome was determined by real-time PCR analysis as previously described [36,42].

3. Results

3.1. Comparison of transduction efficiencies of Ad vectors in WT- and CD46TG-mDCs

First, to compare transduction efficiencies of Ad35 vectors with Ad5 and Ad5F35 vectors in WT- and CD46TG-mDCs, GFP expression in mDCs was analyzed using flow cytometry following Ad vector transduction (Fig. 1). We previously confirmed that CD46TG-mDCs, not WT-mDCs, expressed sufficient levels of human CD46 (data not shown) [34]. In WT-mDCs, Ad5F35GFP and Ad35GFP mediated lower percentages of GFP-positive cells (Ad5GFP; 52%, Ad5F35GFP; 26%, Ad35GFP; 10%) and GFP expression levels (mean fluorescence intensity; MFI) than Ad5-GFP, due to the absence of receptor, CD46, on WT-mDCs (Fig. 1a). In contrast, higher transduction efficiencies of Ad5F35GFP and Ad35GFP were found compared with Ad5GFP in CD46TG-mDCs (GFP-positive cells, Ad5-GFP; 52%, Ad5F35-GFP; 76%, Ad35-GFP; 62%). In both WT-mDCs and CD46TG-mDCs, transduction efficiencies of Ad5F35GFP were higher than those of Ad35GFP (Fig. 1b), probably in part due to the lower infectious-particle titer ratio of Ad35GFP than that of Ad5F35GFP. Ad35 vectors usually have lower PFU-to-particle ratios than Ad5-based vectors [16]. These results indicate that Ad5F35 and Ad35 vectors possess more efficient transduction activity in mDCs expressing human CD46 than Ad5 vectors.

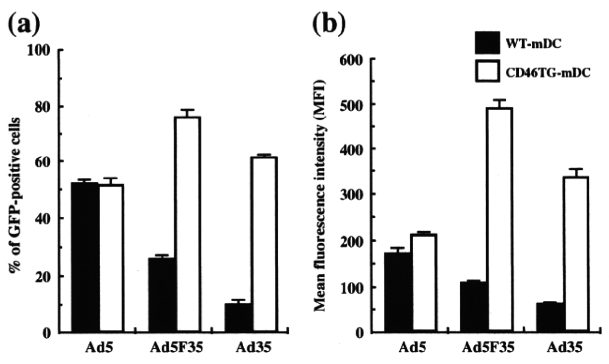

Fig. 1. Transduction efficiencies of Ad vectors in mDCs derived from WT and CD46TG mice. a) Percentages of GFP-positive cells, b) mean fluorescence intensity of GFP. mDCs were transduced with Ad vectors at 3000 VP/cell for 1.5 h. Following 24-h incubation, GFP expression was evaluated by flow cytometry analysis. The data are expressed as means ± S.D. ($n=3$). Each analysis was performed at least twice.

3.2. Surface expression of costimulatory molecules on mDCs following Ad vector transduction

Next, to assess the capacity of Ad5F35 and Ad35 vectors to induce maturation of mDCs, we measured surface expression levels of costimulatory molecules (CD40, CD80, CD86) following Ad vector transduction (Fig. 2). Elevation in expression of costimulatory molecules is crucial for T cell activation. Incubation of WT-mDCs or CD46TG-mDCs with LPS resulted in significant upregulation of CD80 and CD86, indicating that both mDCs have the ability to mature in response to pathogens. WT-mDCs did not show apparent increases in the expression of CD40 or CD80 following Ad vector transduction; however, CD86 expression was elevated by transduction with all types of Ad vectors (Fig. 2a). Ad35GFP induced slightly higher CD86 expression (1.6-fold relative to mock) than Ad5GFP (1.4-fold) and AdF35GFP (1.2-fold).

CD46TG-mDCs exhibited slightly different expression profiles of costimulatory molecules, compared with WT-mDCs, following transduction with Ad vectors (Fig. 2b). CD80 expression was more highly enhanced by transduction with Ad5F35GFP (1.5-fold) or Ad35GFP (2.1-fold), compared with Ad5GFP (1.2-fold). Ad5F35GFP and Ad35GFP also induced 2.3-fold and 2.5-fold increases in CD86 expression in CD46TG-mDCs, respectively, by contrast, 1.9-fold increase in CD86 expression was found after Ad5GFP transduction. These results indicate that Ad35 and Ad5F35 vectors more largely induce maturation of CD46TG-mDCs than Ad5 vectors. Furthermore, Ad35GFP mediated higher levels of CD80 and CD86 expression than Ad5F35GFP in CD46TG-mDCs.

3.3. In vitro induction of inflammatory cytokines and IFN-β following Ad vector transduction in mDCs

To evaluate the ability of Ad5F35 and Ad35 vectors to induce production of inflammatory cytokines and interferons *in vitro*, we measured the levels of IL-6, -12, TNF-α, and IFN-β in the medium by ELISA following Ad vector transduction in mDCs (Fig. 3) As previously demonstrated, transduction with Ad5GFP resulted in enhanced releases of IL-6 and IL-12 in WT-mDCs [43]. However, Ad35GFP induced higher levels of IL-6 and IL-12 than did Ad5GFP. In contrast, IL-6 and IL-12 levels by Ad5F35GFP were almost comparable to mock-transduced levels in WT-mDCs. The apparent induction of IFN-β or TNF-α was not detected following Ad vector transduction.

CD46TG-mDCs produced much larger amounts of these cytokines after transduction with Ad5F35GFP or Ad35GFP than did WT-mDCs. Ad35GFP exhibited 4.2-, 6.4-, 8.0-, and 77.5-fold increases in IL-6, IL-

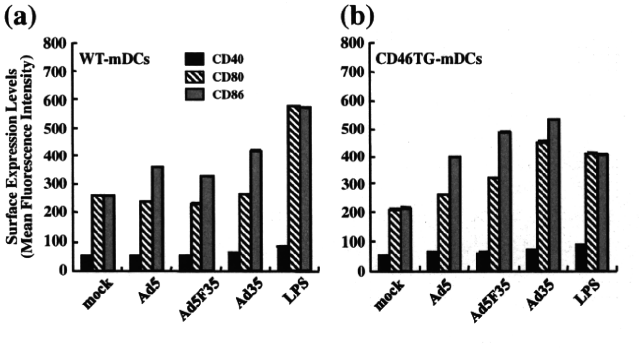

Fig. 2. Surface expression levels of costimulatory molecules on mDCs following Ad vector transduction. a) WT-mDCs, b) CD46TG-mDCs. mDCs were transduced with Ad vectors as described in Fig.1. Following 24-h incubation, cells were stained with monoclonal antibodies, and subsequently analyzed by flow cytomtery as described in "Materials and methods". mDCs were treated with 1 μg/ml LPS for 24 h as a positive control for phenotypical DC maturation. The data are expressed as means ± S.D. ($n=3$). Each analysis was performed at least twice.

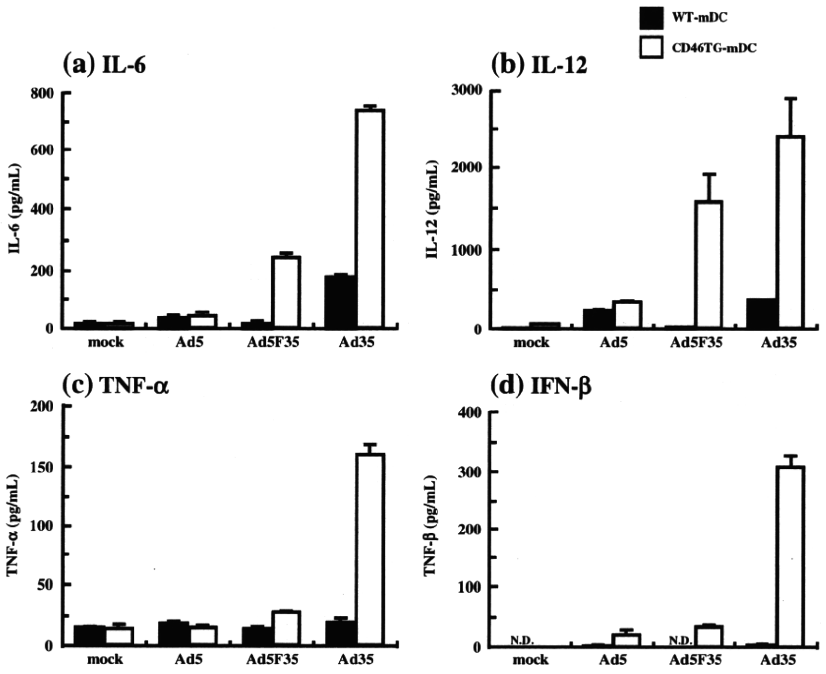

Fig. 3. Production of inflammatory cytokines and IFN-β in WT-mDCs (open bar) and CD46TG-mDCs (closed bar) following Ad vector transduction. a) IL-6, b) IL-12, c) TNF-α, d) IFN-β. mDCs were transduced with Ad vectors as described in Fig. 1. Following 24-h incubation, the culture medium was harvested and the amounts of IL-6, IL-12, TNF-α, and IFN-β in the medium were measured by ELISA. The data are expressed as means ± S.D. ($n = 3$). Each analysis was performed at least twice. N.D.; not detected.

12, TNF-α, and IFN-β compared with WT-mDCs, respectively. Ad5F35GFP induced 14.5-fold and 60.9-fold higher IL-6 and IL-12 production than did WT-mDCs, respectively, although production of IL-6, IL-12, and IFN-β by Ad5GFP was also slightly higher in CD46TG-mDCs than in WT-mDCs. These results indicate that expression of human CD46 enhances transduction with Ad35 and Ad5F35 vectors in mDCs, leading to higher induction of inflammatory cytokines and IFN-β, at least *in vitro*.

3.4. *In vivo* inflammatory cytokine production following intravenous administration of Ad vectors

To evaluate *in vivo* inflammatory cytokine production following systemic administration of Ad vectors, Ad vectors were systemically injected into WT and CD46TG mice, and serum levels of IL-6 and IL-12 were measured 6 h after injection (Fig. 4). We previously confirmed that this CD46TG mouse line ubiquitously expresses human CD46 in a pattern similar to that in humans [34]. Ad5L exhibited IL-6 induction in both WT and CD46TG mice following intravenous administration. However, intravenous administration of Ad35L resulted in 4.4-fold and 3.4-fold higher amounts of IL-6 production in WT and CD46TG mice, respectively, compared with Ad5L (Fig. 4a). We did not find statistically significant difference in IL-6 levels by Ad35L between WT and CD46TG mice, although the average of IL-6 production by Ad35L in WT mice was approximately twice than that in CD46TG mice. These results suggest that expression of human CD46 would not be largely involved in Ad35 vector-induced *in vivo* IL-6 production. In contrast, Ad5F35L, which also recognizes human CD46 as a receptor, elicited lower IL-6 production than Ad35L in both WT and CD46TG mice. The IL-6 level by Ad5F35L was significantly higher than that by PBS in WT mice, whereas there was no statistically significant difference in IL-6 levels between PBS- or Ad5F35L-injected CD46TG mice.

The Ad vector-induced IL-12 production profile *in vivo* was slightly different from that of IL-6 (Fig. 4b). In both WT and CD46TG mice, Ad35L induced IL-12 production to a level almost comparable to that induced by Ad5L. There was no statistically significant difference between IL-12 production by Ad35L in WT and CD46TG mice, suggesting that human CD46 is not involved in Ad35 vector-induced IL-12 production, similarly to the case with IL-6 production. On the other hand, IL-12 production levels by Ad5F35L in WT and CD46TG mice were much lower than those by Ad5L or Ad35L, and were almost comparable to those in mice receiving PBS. These results indicate that

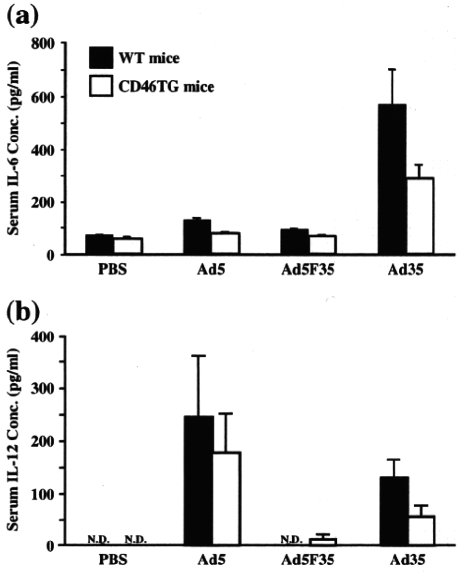

Fig. 4. *In vivo* inflammatory cytokine production following intravenous administration of Ad vectors in WT mice (open bar) and CD46TG mice (closed bar). a) IL-6, b) IL-12. WT and CD46TG mice were intravenously administered with Ad vectors at a dose of 1.5×10^{10} VP/mouse. Six hours post-administration, blood samples were collected via retro-orbital bleeding. Concentrations of inflammatory cytokines were measured by ELISA. The data are expressed as means ± S.D. ($n = 3$–5). Each analysis was performed at least twice. N.D.; not detected.

Ad35 vectors activate inflammatory cytokine production more intensely than do Ad5F35 vectors in WT and CD46TG mice.

3.5. Ad vector accumulation in the spleen following Ad vector injection

Next, real-time PCR analysis was carried out to evaluate the copy number of the Ad vector genome in the spleen. We previously demonstrated that the spleen is involved mainly in Ad vector-induced inflammatory cytokine production [44]. The analysis demonstrated that similar amounts of vector genomes of Ad5L and Ad35L were detected in the spleens of WT and CD46TG mice (Fig. 5). In contrast, the average vector genome copy numbers of Ad5F35L were slightly lower than those of Ad5L and Ad35L in both WT and CD46TG mice, although statistically significant differences were not found. Lower levels of inflammatory cytokine induction by Ad5F35L might be due to the lower levels of accumulation of Ad5F35L in the spleen.

4. Discussion

Innate immune responses by Ad vectors often cause unwanted side effects, including hepatotoxicity and vascular damage. However, when Ad vectors are used as vaccine vectors expressing antigens, Ad vector-induced innate immunity enhances immune responses against the expressed antigens, resulting in higher therapeutic effects. Therefore, the induction properties of innate immunity by Ad vectors should be clarified. Thus far, however, few studies have directly compared transduction properties, including innate immune responses, between Ad5F35 and Ad35 vectors, which are promising as vaccine vectors. The aim of this study was to examine innate immune responses by fiber-substituted Ad5F35 vectors and species B Ad35 vectors, both of which bind to human CD46, in comparison with conventional Ad5 vectors. Our findings revealed that Ad5F35 and Ad35 vectors induce distinct profiles of innate immune responses following transduction.

A main question raised by this study is why Ad35 vectors elicit higher innate immune responses (costimulatory molecule expression and inflammatory cytokine production) than Ad5F35 vectors. A similar phenomenon was found in fiber-substituted Ad5 vectors containing fiber proteins of species B Ad serotype 11 (Ad11) (Ad5F11) and Ad11 vectors, which utilize human CD46. In CD46TG mice, intravenous administration of Ad11 vectors resulted in higher amounts of inflammatory cytokines than did administration of Ad5F11 vectors [45]. Both Ad5F35 and Ad35 vectors possess the same fiber knob and shaft, so other viral components, including the hexon, penton base, and Ad genome, would be involved in the differences in innate immune responses between these Ad vectors. The primary candidate of the key component of inflammatory cytokine induction is the Ad genome. mDCs were induced from bone marrow cells using GM-CSF in this study. We previously demonstrated that GM-CSF-induced mDCs express toll-like receptor (TLR) 9 and that Ad5 vector-mediated inflammatory cytokine induction in GM-CSF-induced mDCs is TLR9-dependent [43]. TLR9 recognizes the unmethylated CpG motif as a ligand for the induction of innate immune responses. The Ad genome might be recognized by TLR9 in mDCs. Iacobelli-Martinez et al. demonstrated that CD46-utilizing Ad vectors activate innate immunity via a TLR9-dependent pathway; however, there are fewer CpG dinucleotides in the Ad35 genome than in the Ad5 genome [46]. Factors other than the number of CpG motifs in Ad genomes might explain the differences in innate immunity between Ad5F35 and Ad35 vectors. In addition, the copy numbers of the Ad35 vector genome were slightly higher than those of Ad5F35L in the spleen. The difference in the vector accumulation of Ad35 and Ad5F35 vectors in the spleen might partly explain the differences in inflammatory cytokine induction following intravenous administration.

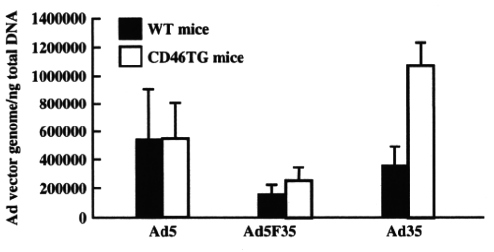

Fig. 5. Ad vector copy numbers in the spleens of WT and CD46TG mice 3 h following intravenous administration. WT and CD46TG mice were intravenously administered with Ad vectors as described in Fig. 4. Three hours post-administration, total DNA, including the Ad vector genome, was isolated from the spleen. The Ad vector genome copy numbers were evaluated by real-time PCR. The data are expressed as means ± S.E. ($n = 3$–5).

In vaccine therapy, it is indispensable to elicit a T-cell response against a vaccine antigen. Because innate immune responses play crucial roles in the induction of acquired immunity, high levels of innate immune responses by Ad35 vectors are beneficial for vaccine therapy application. However, several studies have demonstrated low levels of T-cell responses against antigens expressed by Ad35 vectors in rhesus monkeys [47] and conventional mice [17,48]. It remains unclear why Ad35 vectors induced the low levels of T-cell responses in these studies. On the other hand, Ad35 vector-induced efficient T-cell responses have also been reported [24,49,50]. Various factors, including animals, injection routes, and antigen, would affect the T-cell response levels against antigens delivered by Ad35 vectors.

It is well known that human CD46 serves as a receptor for several pathogens, including human herpesvirus type 6 and measles virus [11,12,51–53]. Due to the limited expression of rodent CD46 in the testis and low homology between human and rodent CD46 [28], human CD46TG mice have often been used in studies of these pathogens as well as in studies elucidating function of human CD46 [29–33]. These studies indicate that CD46TG mice can be used to characterize CD46-utilizing pathogens. We examined the transduction properties of Ad35 vectors in CD46TG mice [34] and cynomologus macaques [54], and did not find obvious differences in transduction properties of Ad35 vectors between the two animals. However, there was no apparent difference in IL-6 levels by Ad5 or Ad35 vectors following systemic injection in cynomologus macaques [54], which differs from the data in this study using CD46TG mice [34]. We should pay attention to the differences in the results between nonhuman primates and CD46TG mice.

We previously reported that the uptake of Ad35 vectors in the organs, including the spleen, was increased in CD46TG mice compared with WT mice 48 h after injection [34], in contrast, similar amounts of Ad35 vector genome were detected in the spleens of both WT and CD46TG mice 3 h after injection in this study. Probably the vector genome of Ad35L which were phagocytosed by macrophages and dendritic cells would be degraded 48 h after injection. The vector genome of Ad35L taken up via a CD46-dependent pathway might remain in the spleen, leading to differences in the amounts of Ad35L genome in the spleens of WT and CD46TG mice 48 h after injection in the previous study [34]. We previously demonstrated that Ad vector genome taken up by liver Kupffer cells was detected by PCR 1 h after Ad vector injection, but was clearly degraded 48 h after injection [39].

Previous studies, including ours, have demonstrated that spleen dendritic cells play a crucial role in inflammatory cytokine production following the systemic injection of Ad vectors [44,55–58]. In the present study, we found similar amounts of Ad35 vector genome in the spleens of WT and CD46TG mice 3 h after injection. These results would explain that there were not statistically significant differences in IL-6 or IL-12 production by Ad35 vectors between WT and CD46TG mice. As described above, larger amount of Ad35 vector genome detected in the spleen of CD46TG mice than that of WT mice 48 h after injection would be due to the high level of human CD46 expression in

CD46TG mice, suggesting that the human CD46-dependent uptake of Ad35 vectors in the spleen would not be largely involved in *in vivo* inflammatory cytokine production. The uptake of Ad35 vectors by spleen dendritic cells via phagocytosis, not CD46-dependent endocytosis, would be mainly responsible for *in vivo* inflammatory cytokine production. In the present study, the induction level of IL-6 in mice receiving Ad5 vectors was lower than that in our previous study, probably due to the higher dose of Ad5 vectors used in the previous study [43]. A higher level of IL-6 induction was found at a higher dose of Ad5GFP (data not shown).

In conclusion, we have demonstrated that Ad35 vectors are better than Ad5F35 vectors at inducing innate immune responses in mDCs expressing human CD46 and CD46TG mice, even though both Ad vectors utilize the same receptor. This study also exhibits important clues for the elucidation of the mechanism underlying Ad vector-mediated innate immune responses, as well as the utility of CD46TG mice as an animal model for Ad5F35 and Ad35 vectors.

Acknowledgments

We thank Dr. Masaru Okabe (Osaka University, Osaka, Japan) for kindly providing the CD46TG mice. This work was supported by a grant for Research on Publicly Essential Drugs and Medical Devices from the Japan Health Sciences Foundation and a Grant-in-Aid for Scientific Research on Priority Areas from the Ministry of Education, Culture, Sports, Science, and Technology (MEXT) of Japan.

References

[1] N. Okada, T. Saito, Y. Masunaga, Y. Tsukada, S. Nakagawa, H. Mizuguchi, K. Mori, Y. Okada, T. Fujita, T. Hayakawa, T. Mayumi, A. Yamamoto, Efficient antigen gene transduction using Arg-Gly-Asp fiber-mutant adenovirus vectors can potentiate antitumor vaccine efficacy and maturation of murine dendritic cells, Cancer Res. 61 (2001) 7913–7919.

[2] T.D. de Gruijl, O.J. Ophorst, J. Goudsmit, S. Verhaagh, S.M. Lougheed, K. Radosevic, M.J. Havenga, R.J. Scheper, Intradermal delivery of adenoviral type-35 vectors leads to high efficiency transduction of mature, CD8+ T cell-stimulating skin-emigrated dendritic cells, J. Immunol. 177 (2006) 2208–2215.

[3] N. Kanagawa, R. Koretomo, S. Murakami, F. Sakurai, H. Mizuguchi, S. Nakagawa, T. Fujita, A. Yamamoto, N. Okada, Factors involved in the maturation of murine dendritic cells transduced with adenoviral vector variants, Virology 374 (2008) 411–420.

[4] D. Rea, M.J. Havenga, M. van Den Assem, R.P. Sutmuller, A. Lemckert, R.C. Hoeben, A. Bout, C.J. Melief, R. Offringa, Highly efficient transduction of human monocyte-derived dendritic cells with subgroup B fiber-modified adenovirus vectors enhances transgene-encoded antigen presentation to cytotoxic T cells, J. Immunol. 166 (2001) 5236–5244.

[5] K.L. O'Brien, J. Liu, S.L. King, Y.H. Sun, J.E. Schmitz, M.A. Lifton, N.A. Hutnick, M.R. Betts, S.A. Dubey, J. Goudsmit, J.W. Shiver, M.N. Robertson, D.R. Casimiro, D.H. Barouch, Adenovirus-specific immunity after immunization with an Ad5 HIV-1 vaccine candidate in humans, Nat. Med. 15 (2009) 873–875.

[6] R.A. Koup, L. Lamoreaux, D. Zarkowsky, R.T. Bailer, C.R. King, J.G. Gall, D.E. Brough, B.S. Graham, M. Roederer, Replication-defective adenovirus vectors with multiple deletions do not induce measurable vector-specific T cells in human trials, J. Virol. 83 (2009) 6318–6322.

[7] J. Liu, K.L. O'Brien, D.M. Lynch, N.L. Simmons, A. La Porte, A.M. Riggs, P. Abbink, R.T. Coffey, L.E. Grandpre, M.S. Seaman, G. Landucci, D.N. Forthal, D.C. Montefiori, A. Carville, K.G. Mansfield, M.J. Havenga, M.G. Pau, J. Goudsmit, D.H. Barouch, Immune control of an SIV challenge by a T-cell-based vaccine in rhesus monkeys, Nature 457 (2009) 87–91.

[8] H. Mizuguchi, T. Hayakawa, Adenovirus vectors containing chimeric type 5 and type 35 fiber proteins exhibit altered and expanded tropism and increase the size limit of foreign genes, Gene 285 (2002) 69–77.

[9] D.M. Shayakhmetov, T. Papayannopoulou, G. Stamatoyannopoulos, A. Lieber, Efficient gene transfer into human CD34(+) cells by a retargeted adenovirus vector, J. Virol. 74 (2000) 2567–2583.

[10] H. Stecher, D.M. Shayakhmetov, G. Stamatoyannopoulos, A. Lieber, A capsid-modified adenovirus vector devoid of all viral genes: assessment of transduction and toxicity in human hematopoietic cells, Mol. Ther. 4 (2001) 36–44.

[11] A. Segerman, J.P. Atkinson, M. Marttila, V. Dennerquist, G. Wadell, N. Arnberg, Adenovirus type 11 uses CD46 as a cellular receptor, J. Virol. 77 (2003) 9183–9191.

[12] A. Gaggar, D.M. Shayakhmetov, A. Lieber, CD46 is a cellular receptor for group B adenoviruses, Nat. Med. 9 (2003) 1408–1412.

[13] O.J. Ophorst, S. Kostense, J. Goudsmit, R.L. De Swart, S. Verhaagh, A. Zakhartchouk, M. Van Meijer, M. Sprangers, G. Van Amerongen, S. Yuksel, A.D. Osterhaus, M.J. Havenga, An adenoviral type 5 vector carrying a type 35 fiber as a vaccine vehicle: DC targeting, cross neutralization, and immunogenicity, Vaccine 22 (2004) 3035–3044.

[14] L. Holterman, R. Vogels, R. van der Vlugt, M. Sieuwerts, J. Grimbergen, J. Kaspers, E. Geelen, E. van der Helm, A. Lemckert, G. Gillissen, S. Verhaagh, J. Custers, D. Zuijdgeest, B. Berkhout, M. Bakker, P. Quax, J. Goudsmit, M. Havenga, Novel replication-incompetent vector derived from adenovirus type 11 (Ad11) for vaccination and gene therapy: low seroprevalence and non-cross-reactivity with Ad5, J. Virol. 78 (2004) 13207–13215.

[15] D. Stone, S. Ni, Z.Y. Li, A. Gaggar, N. DiPaolo, Q. Feng, V. Sandig, A. Lieber, Development and assessment of human adenovirus type 11 as a gene transfer vector, J. Virol. 79 (2005) 5090–5104.

[16] F. Sakurai, H. Mizuguchi, T. Hayakawa, Efficient gene transfer into human CD34+ cells by an adenovirus type 35 vector, Gene Ther. 10 (2003) 1041–1048.

[17] D.H. Barouch, M.G. Pau, J.H. Custers, W. Koudstaal, S. Kostense, M.J. Havenga, D.M. Truitt, S.M. Sumida, M.G. Kishko, J.C. Arthur, B. Korioth-Schmitz, M.H. Newberg, D.A. Gorgone, M.A. Lifton, D.L. Panicali, G.J. Nabel, N.L. Letvin, J. Goudsmit, Immunogenicity of recombinant adenovirus serotype 35 vaccine in the presence of pre-existing anti-Ad5 immunity, J. Immunol. 172 (2004) 6290–6297.

[18] A.A. Lemckert, S.M. Sumida, L. Holterman, R. Vogels, D.M. Truitt, D.M. Lynch, A. Nanda, B.A. Ewald, D.A. Gorgone, M.A. Lifton, J. Goudsmit, M.J. Havenga, D.H. Barouch, Immunogenicity of heterologous prime-boost regimens involving recombinant adenovirus serotype 11 (Ad11) and Ad35 vaccine vectors in the presence of anti-ad5 immunity, J. Virol. 79 (2005) 9694–9701.

[19] M.J. Havenga, A.A. Lemckert, O.J. Ophorst, M. van Meijer, W.T. Germeraad, J. Grimbergen, M.A. van Den Doel, R. Vogels, J. van Deutekom, A.A. Janson, J.D. de Bruijn, F. Uytdehaag, P.H. Quax, T. Logtenberg, M. Mehtali, A. Bout, Exploiting the natural diversity in adenovirus tropism for therapy and prevention of disease, J. Virol. 76 (2002) 4612–4620.

[20] R. Vogels, D. Zuijdgeest, R. van Rijnsoever, E. Hartkoorn, I. Damen, M.P. de Bethune, S. Kostense, G. Penders, N. Helmus, W. Koudstaal, M. Cecchini, A. Wetterwald, M. Sprangers, A. Lemckert, O. Ophorst, B. Koel, M. van Meerendonk, P. Quax, L. Panitti, J. Grimbergen, A. Bout, J. Goudsmit, M. Havenga, Replication-deficient human adenovirus type 35 vectors for gene transfer and vaccination: efficient human cell infection and bypass of preexisting adenovirus immunity, J. Virol. 77 (2003) 8263–8271.

[21] E. Nwanegbo, E. Vardas, W. Gao, H. Whittle, H. Sun, D. Rowe, P.D. Robbins, A. Gambotto, Prevalence of neutralizing antibodies to adenoviral serotypes 5 and 35 in the adult populations of The Gambia, South Africa, and the United States, Clin Diagn Lab Immunol 11 (2004) 351–357.

[22] N. DiPaolo, S. Ni, A. Gaggar, R. Strauss, S. Tuve, Z.Y. Li, D. Stone, D. Shayakhmetov, N. Kiviat, P. Toure, S. Sow, B. Horvat, A. Lieber, Evaluation of adenovirus vectors containing serotype 35 fibers for vaccination, Mol. Ther. 13 (2006) 756–765.

[23] H.B. Wang, A. Kondo, A. Yoshida, S. Yoshizaki, S. Abe, L.L. Bao, N. Mizuki, M. Ichino, D. Klinman, K. Okuda, M. Shimada, Partial protection against SIV challenge by vaccination of adenovirus and MVA vectors in rhesus monkeys, Gene Ther, (2010) 17 4-13.

[24] A. Rodriguez, R. Mintardjo, D. Tax, G. Gillissen, J. Custers, M.G. Pau, J. Klap, S. Santra, H. Balachandran, N.L. Letvin, J. Goudsmit, K. Radosevic, Evaluation of a prime-boost vaccine schedule with distinct adenovirus vectors against malaria in rhesus monkeys, Vaccine 27 (2009) 6226–6233.

[25] A.C. Soloff, X. Liu, W. Gao, R.D. Day, A. Gambotto, S.M. Barratt-Boyes, Adenovirus 5- and 35-based immunotherapy enhances the strength but not breadth or quality of immunity during chronic SIV infection, Eur. J. Immunol. 39 (2009) 2437–2449.

[26] I. Magalhaes, D.R. Sizemore, R.K. Ahmed, S. Mueller, L. Wehlin, C. Scanga, F. Weichold, G. Schirru, M.G. Pau, J. Goudsmit, S. Kuhlmann-Berenzon, M. Spangberg, J. Andersson, H. Gaines, R. Thorstensson, Y.A. Skeiky, J. Sadoff, M. Maeurer, rBCG induces strong antigen-specific T cell responses in rhesus macaques in a prime-boost setting with an adenovirus 35 tuberculosis vaccine vector, PLoS ONE 3 (2008) e3790.

[27] M. Shimada, H.B. Wang, A. Kondo, X.P. Xu, A. Yoshida, K. Shinoda, T. Ura, H. Mizuguchi, D. Klinman, J.L. Luo, H. Bai, K. Okuda, Effect of therapeutic immunization using Ad5/35 and MVA vectors on SIV infection of rhesus monkeys undergoing antiretroviral therapy, Gene Ther. 16 (2009) 218–228.

[28] A. Tsujimura, K. Shida, M. Kitamura, M. Nomura, J. Takeda, H. Tanaka, M. Matsumoto, K. Matsumiya, A. Okuyama, Y. Nishimune, M. Okabe, T. Seya, Molecular cloning of a murine homologue of membrane cofactor protein (CD46): preferential expression in testicular germ cells, Biochem. J. 330 (Pt 1) (1998) 163–168.

[29] M. Shingai, N. Inoue, T. Okuno, M. Okabe, T. Akazawa, Y. Miyamoto, M. Ayata, K. Honda, M. Kurita-Taniguchi, M. Matsumoto, H. Ogura, T. Taniguchi, T. Seya, Wild-type measles virus infection in human CD46/CD150-transgenic mice: CD11c-positive dendritic cells establish systemic viral infection, J. Immunol. 175 (2005) 3252–3261.

[30] J.C. Marie, J. Kehren, M.C. Trescol-Biemont, A. Evlashev, H. Valentin, T. Walzer, R. Tedone, B. Loveland, J.F. Nicolas, C. Rabourdin-Combe, B. Horvat, Mechanism of measles virus-induced suppression of inflammatory immune responses, Immunity 14 (2001) 69–79.

[31] L. Johansson, A. Rytkonen, H. Wan, P. Bergman, L. Plant, B. Agerberth, T. Hokfelt, A. B. Jonsson, Human-like immune responses in CD46 transgenic mice, J. Immunol. 175 (2005) 433–440.

[32] L. Johansson, A. Rytkonen, P. Bergman, B. Albiger, H. Kallstrom, T. Hokfelt, B. Agerberth, R. Cattaneo, A.B. Jonsson, CD46 in meningococcal disease, Science 301 (2003) 373–375.

[33] H. Matsui, Y. Sekiya, M. Nakamura, S.Y. Murayama, H. Yoshida, T. Takahashi, K. Imanishi, K. Tsuchimoto, T. Uchiyama, K. Sunakawa, K. Ubukata, CD46 transgenic

mouse model of necrotizing fasciitis caused by *Streptococcus pyogenes* infection, Infect. Immun. 77 (2009) 4806–4814.
[34] F. Sakurai, K. Kawabata, N. Koizumi, N. Inoue, M. Okabe, T. Yamaguchi, T. Hayakawa, H. Mizuguchi, Adenovirus serotype 35 vector-mediated transduction into human CD46-transgenic mice, Gene Ther. 13 (2006) 1118–1126.
[35] M.B. Lutz, N. Kukutsch, A.L. Ogilvie, S. Rossner, F. Koch, N. Romani, G. Schuler, An advanced culture method for generating large quantities of highly pure dendritic cells from mouse bone marrow, J Immunol Methods 223 (1999) 77–92.
[36] F. Sakurai, K. Kawabata, T. Yamaguchi, T. Hayakawa, H. Mizuguchi, Optimization of adenovirus serotype 35 vectors for efficient transduction in human hematopoietic progenitors: comparison of promoter activities, Gene Ther. 12 (2005) 1424–1433.
[37] H. Mizuguchi, M.A. Kay, Efficient construction of a recombinant adenovirus vector by an improved in vitro ligation method, Hum. Gene Ther. 9 (1998) 2577–2583.
[38] H. Mizuguchi, M.A. Kay, A simple method for constructing E1- and E1/E4-deleted recombinant adenoviral vectors, Hum. Gene Ther. 10 (1999) 2013–2017.
[39] F. Sakurai, H. Mizuguchi, T. Yamaguchi, T. Hayakawa, Characterization of in vitro and in vivo gene transfer properties of adenovirus serotype 35 vector, Mol. Ther. 8 (2003) 813–821.
[40] J.V. Maizel Jr., D.O. White, M.D. Scharff, The polypeptides of adenovirus. I. Evidence for multiple protein components in the virion and a comparison of types 2, 7A, and 12, Virology 36 (1968) 115–125.
[41] Y. Kanegae, M. Makimura, I. Saito, A simple and efficient method for purification of infectious recombinant adenovirus, Jpn J. Med. Sci. Biol. 47 (1994) 157–166.
[42] N. Koizumi, K. Kawabata, F. Sakurai, Y. Watanabe, T. Hayakawa, H. Mizuguchi, Modified adenoviral vectors ablated for coxsackievirus-adenovirus receptor, alphav integrin, and heparan sulfate binding reduce in vivo tissue transduction and toxicity, Hum. Gene Ther. 17 (2006) 264–279.
[43] T. Yamaguchi, K. Kawabata, N. Koizumi, F. Sakurai, K. Nakashima, H. Sakurai, T. Sasaki, N. Okada, K. Yamanishi, H. Mizuguchi, Role of MyD88 and TLR9 in the innate immune response elicited by serotype 5 adenoviral vectors, Hum. Gene Ther. 18 (2007) 753–762.
[44] N. Koizumi, T. Yamaguchi, K. Kawabata, F. Sakurai, T. Sasaki, Y. Watanabe, T. Hayakawa, H. Mizuguchi, Fiber-modified adenovirus vectors decrease liver toxicity through reduced IL-6 production, J. Immunol. 178 (2007) 1767–1773.
[45] D. Stone, Y. Liu, Z.Y. Li, S. Tuve, R. Strauss, A. Lieber, Comparison of adenoviruses from species B, C, e, and f after intravenous delivery, Mol Ther 15 (2007) 2146–2153.
[46] M. Iacobelli-Martinez, G.R. Nemerow, Preferential activation of Toll-like receptor nine by CD46-utilizing adenoviruses, J. Virol. 81 (2007) 1305–1312.
[47] A. Nanda, D.M. Lynch, J. Goudsmit, A.A. Lemckert, B.A. Ewald, S.M. Sumida, D.M. Truitt, P. Abbink, M.G. Kishko, D.A. Gorgone, M.A. Lifton, L. Shen, A. Carville, K.G. Mansfield, M.J. Havenga, D.H. Barouch, Immunogenicity of recombinant fiber-chimeric adenovirus serotype 35 vector-based vaccines in mice and rhesus monkeys, J. Virol. 79 (2005) 14161–14168.
[48] A.R. Thorner, A.A. Lemckert, J. Goudsmit, D.M. Lynch, B.A. Ewald, M. Denholtz, M.J. Havenga, D.H. Barouch, Immunogenicity of heterologous recombinant adenovirus prime-boost vaccine regimens is enhanced by circumventing vector cross-reactivity, J. Virol. 80 (2006) 12009–12016.
[49] O.J. Ophorst, K. Radosevic, M.J. Havenga, M.G. Pau, L. Holterman, B. Berkhout, J. Goudsmit, M. Tsuji, Immunogenicity and protection of a recombinant human adenovirus serotype 35-based malaria vaccine against *Plasmodium yoelii* in mice, Infect. Immun. 74 (2006) 313–320.
[50] J.P. Shott, S.M. McGrath, M.G. Pau, J.H. Custers, O. Ophorst, M.A. Demoitie, M.C. Dubois, J. Komisar, M. Cobb, K.E. Kester, P. Dubois, J. Cohen, J. Goudsmit, D.G. Heppner, V.A. Stewart, Adenovirus 5 and 35 vectors expressing *Plasmodium falciparum* circumsporozoite surface protein elicit potent antigen-specific cellular IFN-gamma and antibody responses in mice, Vaccine 26 (2008) 2818–2823.
[51] R. Cattaneo, Four viruses, two bacteria, and one receptor: membrane cofactor protein (CD46) as pathogens' magnet, J. Virol. 78 (2004) 4385–4388.
[52] R.E. Dorig, A. Marcil, A. Chopra, C.D. Richardson, The human CD46 molecule is a receptor for measles virus (Edmonston strain), Cell 75 (1993) 295–305.
[53] F. Santoro, P.E. Kennedy, G. Locatelli, M.S. Malnati, E.A. Berger, P. Lusso, CD46 is a cellular receptor for human herpesvirus 6, Cell 99 (1999) 817–827.
[54] F. Sakurai, S. Nakamura, K. Akitomo, H. Shibata, K. Terao, K. Kawabata, T. Hayakawa, H. Mizuguchi, Transduction properties of adenovirus serotype 35 vectors after intravenous administration into nonhuman primates, Mol. Ther. 16 (2008) 726–733.
[55] Y. Zhang, N. Chirmule, G.P. Gao, R. Qian, M. Croyle, B. Joshi, J. Tazelaar, J.M. Wilson, Acute cytokine response to systemic adenoviral vectors in mice is mediated by dendritic cells and macrophages, Mol. Ther. 3 (2001) 697–707.
[56] H. Sakurai, K. Tashiro, K. Kawabata, T. Yamaguchi, F. Sakurai, S. Nakagawa, H. Mizuguchi, Adenoviral expression of suppressor of cytokine signaling-1 reduces adenovirus vector-induced innate immune responses, J. Immunol. 180 (2008) 4931–4938.
[57] B. De Geest, J. Snoeys, S. Van Linthout, J. Lievens, D. Collen, Elimination of innate immune responses and liver inflammation by PEGylation of adenoviral vectors and methylprednisolone, Hum. Gene Ther. 16 (2005) 1439–1451.
[58] H. Sakurai, K. Kawabata, F. Sakurai, S. Nakagawa, H. Mizuguchi, Innate immune response induced by gene delivery vectors, Int. J. Pharm. 354 (2008) 9–15.

© The American Society of Gene & Cell Therapy
MTOpen

Efficient Generation of Hepatoblasts From Human ES Cells and iPS Cells by Transient Overexpression of Homeobox Gene *HEX*

Mitsuru Inamura[1,2], Kenji Kawabata[2,3], Kazuo Takayama[1,2], Katsuhisa Tashiro[2], Fuminori Sakurai[2], Kazufumi Katayama[1,2], Masashi Toyoda[4], Hidenori Akutsu[4], Yoshitaka Miyagawa[5], Hajime Okita[5], Nobutaka Kiyokawa[5], Akihiro Umezawa[4], Takao Hayakawa[6,7], Miho K Furue[8,9] and Hiroyuki Mizuguchi[1,2]

[1]Department of Biochemistry and Molecular Biology, Graduate School of Pharmaceutical Sciences, Osaka University, Osaka, Japan; [2]Laboratory of Stem Cell Regulation, National Institute of Biomedical Innovation, Osaka, Japan; [3]Department of Biomedical Innovation, Graduate School of Pharmaceutical Science, Osaka University, Osaka, Japan; [4]Department of Reproductive Biology, National Institute for Child Health and Development, Tokyo, Japan; [5]Department of Developmental Biology and Pathology, National Institute for Child Health and Development, Tokyo, Japan; [6]Pharmaceutics and Medical Devices Agency, Tokyo, Japan; [7]Pharmaceutical Research and Technology Institute, Kinki University, Osaka, Japan; [8]JCRB Cell Bank/Laboratory of Cell Culture, Department of Disease Bioresource, National Institute of Biomedical Innovation, Osaka, Japan; [9]Laboratory of Cell Processing, Institute for Frontier Medical Sciences, Kyoto University, Kyoto, Japan

Human embryonic stem cells (ESCs) and induced pluripotent stem cells (iPSCs) have the potential to differentiate into all cell lineages, including hepatocytes, *in vitro*. Induced hepatocytes have a wide range of potential application in biomedical research, drug discovery, and the treatment of liver disease. However, the existing protocols for hepatic differentiation of PSCs are not very efficient. In this study, we developed an efficient method to induce hepatoblasts, which are progenitors of hepatocytes, from human ESCs and iPSCs by overexpression of the *HEX* gene, which is a homeotic gene and also essential for hepatic differentiation, using a HEX-expressing adenovirus (Ad) vector under serum/feeder cell-free chemically defined conditions. Ad-HEX-transduced cells expressed α-fetoprotein (AFP) at day 9 and then expressed albumin (ALB) at day 12. Furthermore, the Ad-HEX-transduced cells derived from human iPSCs also produced several cytochrome P450 (CYP) isozymes, and these P450 isozymes were capable of converting the substrates to metabolites and responding to the chemical stimulation. Our differentiation protocol using Ad vector-mediated transient HEX transduction under chemically defined conditions efficiently generates hepatoblasts from human ESCs and iPSCs. Thus, our methods would be useful for not only drug screening but also therapeutic applications.

Received 18 March 2010; accepted 13 October 2010; published online 23 November 2010. doi:10.1038/mt.2010.241

INTRODUCTION

Human embryonic stem cells (ESCs) and induced pluripotent stem cells (iPSCs) are able to replicate indefinitely and differentiate into most cell types of the body,[1–4] and thereby have the potential to provide an unlimited source of cells for a variety of applications.[5] Hepatocytes are useful cells for biomedical research, regenerative medicine, and drug discovery. They are particularly applicable to drug screenings, such as for the determination of metabolic and toxicological properties of drug compounds in *in vitro* models, because the liver is the main detoxification organ in the body.[6] For these applications, it is necessary to prepare a large number of functional hepatocytes from human ESCs and iPSCs. Many of the existing methods for cell differentiation of human ESCs and iPSCs into hepatocytes employ undefined, serum-containing medium and feeder cells.[7–9] Preparation of human ESC- and iPSC-derived hepatocytes for therapeutic applications and drug toxicity testing in humans should be done in nonxenogenic culture systems to avoid potential contamination with pathogens. Furthermore, the efficiency of the differentiation of the human ESCs and iPSCs into hepatocytes is not particularly high using these methods.[9–14]

In vertebrate development, the liver is derived from the primitive gut tube, which is formed by a flat sheet of cells called the definitive endoderm.[5,15] Shortly afterwards, the definitive endoderm is separated into endoderm derivatives containing the liver bud, the cells of which are referred to as hepatoblasts. The hepatoblasts have the potential to proliferate and differentiate into both hepatocytes and cholangiocytes. In the process of hepatic differentiation, the maturation is characterized by the expression of liver- and stage-specific genes. For example, α-fetoprotein (AFP) is an early hepatic marker, which is expressed in hepatoblasts in the liver bud until birth, and its expression is dramatically reduced after birth.[16] In contrast, albumin (ALB), which is the most abundant protein synthesized by hepatocytes, is initially expressed at lower levels in early fetal hepatocytes, but its expression level is increased as the hepatocytes mature, reaching a maximum in adult hepatocytes.[17] Furthermore, isoforms of cytochrome P450 (CYP) proteins also exhibit differential expression levels according to the developmental stages

Correspondence: *Hiroyuki Mizuguchi, Department of Biochemistry and Molecular Biology, Graduate School of Pharmaceutical Sciences, Osaka University, 1-6 Yamadaoka, Suita, Osaka 565-0871, Japan. E-mail: mizuguch@phs.osaka-u.ac.jp*

© The American Society of Gene & Cell Therapy

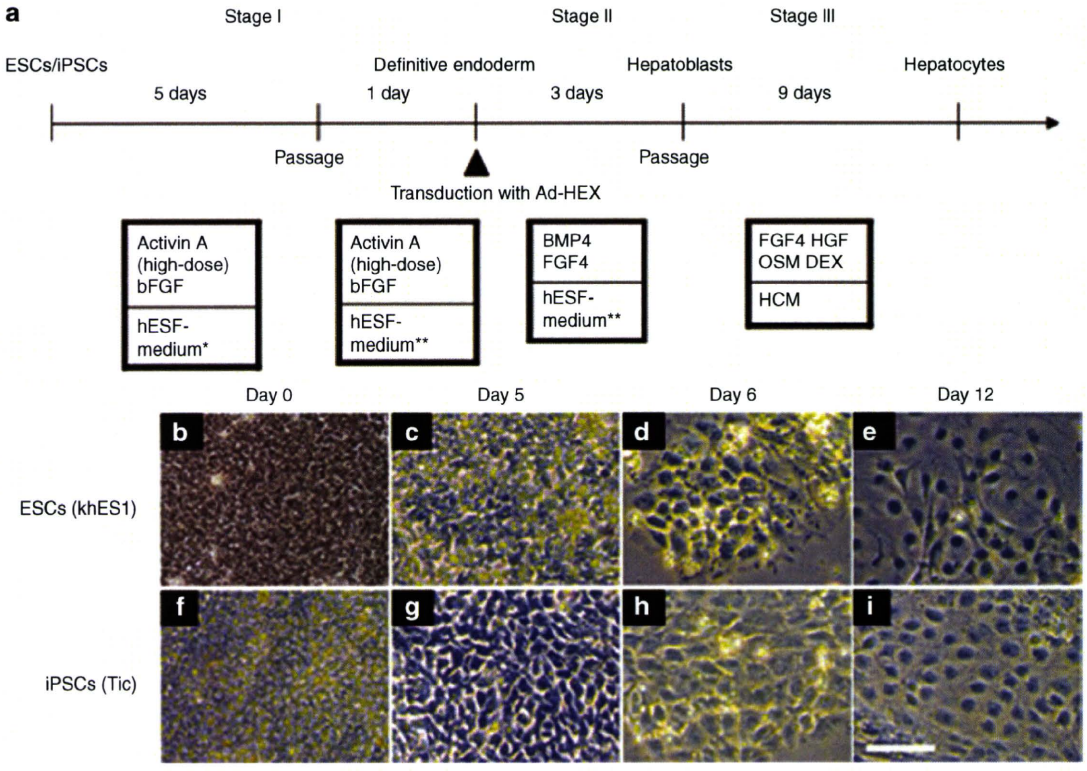

Figure 1 A strategy of differentiation of human embryonic stem cells (ESCs) and induced pluripotent stem cells (iPSCs) to hepatoblasts and hepatocytes. (**a**) Schematic representation illustrating the procedure for differentiation of human ESCs (khES1) and iPSCs (Tic) to hepatocytes. (**b–i**) Phase contrast microscopy showing sequential morphological changes (day 0–12) from (**b–e**) human ESCs (khES1) and (**f–i**) iPSCs (Tic) to hepatoblasts via the definitive endoderm. Bar = 50 μm. bFGF, basic fibroblast growth factor; BMP4, bone morphogenetic protein 4; DEX, dexamethasone; FGF4, fibroblast growth factor 4; HGF, hepatocyte growth factor; OSM, Oncostatin M; HCM, hepatocytes culture medium; *, hESF-GRO medium that was supplemented with 10 μg/ml human recombinant insulin, 5 μg/ml human apotransferrin, 10 μmol/l 2-mercaptoethanol, 10 μmol/l ethanolamine, 10 μmol/l sodium selenite, 0.5 mg/ml fatty acid free BSA; **, hESF-DIF medium that was supplemented with 10 μg/ml insulin, 5 μg/ml apotransferrin, 10 μmol/l 2-mercaptoethanol, 10 μmol/l ethanolamine, 10 μmol/l sodium selenite, 0.5 mg/ml BSA.

of the liver. Although most CYPs (including CYP3A4, CYP7A1, and CYP2D6) are only slightly expressed or not detected in the fetal liver tissue, the expression levels are dramatically increased after birth.[18]

For the development of hepatoblasts, numerous transcription factors are required, such as hematopoietically expressed homeobox (*HEX*), GATA-binding protein 6, prospero homeobox 1, and hepatocyte nuclear factor 4A.[15,19] Among them, *HEX* is suggested to function at the earliest stage of hepatic linage.[20] HEX is first expressed in the definitive endoderm and becomes restricted to the future hepatoblasts. Targeted deletion of the *HEX* gene in the mouse results in embryonic lethality and a dramatic loss of the fetal liver parenchyma.[19,21,22] The hepatic genes, including *ALB*, prospero homeobox1, and hepatocyte nuclear factor 4A, are transiently expressed in the definitive endoderm of *HEX*-null embryos, and further morphogenesis of the hepatoblasts does not occur.[23] In general, then, *HEX* is essential for the definitive endoderm to adopt a hepatic cell fate.

Adenovirus (Ad) vectors are one of the most efficient gene delivery vehicles and have been widely used in both experimental studies and clinical trials.[24] Ad vectors are attractive vehicles for gene transfer because they are easily constructed, can be prepared in high titers, and provide high transduction efficiency in both dividing and nondividing cells. We have developed efficient methods for Ad vector-mediated transient transduction into mouse ESCs and iPSCs.[25,26] We have also showed that the differentiations of mouse ESCs and iPSCs into adipocytes and osteoblasts were dramatically promoted by Ad vector-mediated peroxisome proliferator activated receptor γ and runt related transcription factor 2 transduction, respectively.[25,26]

In this study, we hypothesized that transient *HEX* transduction could efficiently induce hepatoblasts from human ESCs and iPSCs. A previous study demonstrated that *HEX* regulates the differentiation of hemangioblasts and endothelial cells from mouse ESCs,[27] whereas the role of *HEX* in the differentiation of hepatoblasts from human ESCs and iPSCs remains unknown. We found that differentiation of hepatoblasts from the human ESC- and iPSC-derived definitive endoderms, but not from undifferentiated human ESCs and iPSCs, could be facilitated by Ad vector-mediated transient transduction of a *HEX* gene. Furthermore, the Ad-HEX-transduced cells that were derived from human iPSCs were able to differentiate into functional hepatocytes *in vitro*. All the processes for cellular differentiation were performed under serum/feeder cell- free chemically defined conditions. Our culture systems and differentiation method based on Ad vector-mediated transient transduction under chemically defined conditions would provide a platform for drug screening as well as safe therapies.

© The American Society of Gene & Cell Therapy

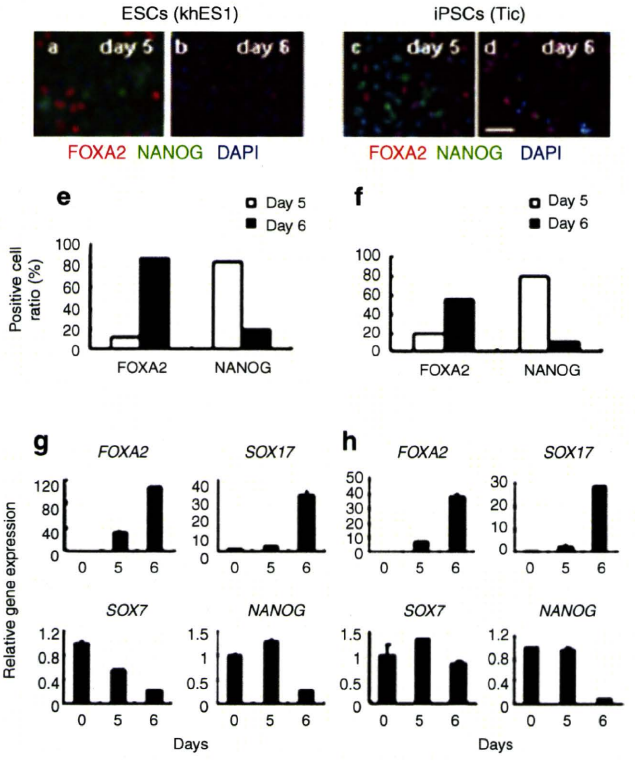

Figure 2 Characterization of the human ESC (khES1)- and iPSC (Tic) derived definitive endoderms. **(a–d)** The immunofluorescent staining of the human ESC (khES1)- and iPSC (Tic) derived differentiated cells before (**a** and **c**; day 5) and after passaging (**b** and **d**; day 6). The cells were immunostained with antibodies against FOXA2 and NANOG. Nuclei were stained with DAPI. **(e,f)** Semiquantitative analysis of the immunofluorescent staining in **a–d**. Data are presented as the mean of immunopositive cells counted in eight independent fields. **(g,h)** Real-time RT-PCR analysis of the level of definitive endoderm (*FOXA2* and *SOX17*), pluripotent (*NANOG*), and extra-embryonic endoderm (*SOX7*) gene expression at day 5 and 6. At day 5, the cells were passaged. Therefore, the data at day 5 and 6 show the levels of gene expression before (at day 5) or after the passage (at day 6). Data are presented as the mean ± SD from triplicate experiments. The graphs represent the relative gene expression level when the level of undifferentiated cells at day 0 was taken as 1. Bar = 50 μm. ESC, embryonic stem cells; iPSC, induced pluripotent stem cells.

RESULTS

Differentiation of human ESC- and iPSC-derived definitive endoderms

Our three-step differentiation protocol is illustrated in Figure 1a. After treatment with 50 ng/ml of Activin A (high-dose) and basic fibroblast growth factor (bFGF) for 5 days on a laminin-coated plate, morphologically, the human ESCs and iPSCs were gradually transformed from typical, defined, tight human ESC, and iPSC colonies (day 0) into less dense, flatter cells containing prominent nuclei (day 5), even though the majority of the cells had a morphology resembling that of undifferentiated cells (Figure 1b,c,f,g). FACS analysis showed that ~46% of human iPSC-derived differentiated cells expressed CXCR4 (expressed in the definitive endoderm but not the primitive endoderm) (**Supplementary Figure S1a**). Human ESC- and iPSC-derived differentiated cells were immunostained with the definitive endoderm marker, FOXA2 (Figure 2a,c). However, the majority of the cells expressed the pluripotent marker NANOG, indicating that undifferentiated cells remain in the induced cultures at day 5. After the cells were passaged with trypsin-EDTA and seeded on a laminin-coated plate a second time, the resultant cells were found to be more homogeneous and flatter at day 6 (Figure 1d,h). Semiquantitative analysis by counting immunopositive cells revealed that the number of FOXA2-positive cells was increased and, in turn, the number of NANOG-positive cells was decreased at day 6 after passaging (Figure 2e,f). Real-time reverse transcriptase (RT)-PCR analysis showed that the definitive endoderm markers *FOXA2* and *SOX17* mRNA were upregulated, whereas the pluripotent marker *NANOG* mRNA was downregulated at day 6 (Figure 2g,h). These results were consistent with the immunofluorescence results (Figure 2a–d). The expression levels of the mesoderm marker *FLK1* mRNA and ectoderm marker *PAX6* mRNA were downregulated or unchanged at day 6 (**Supplementary Figure S1b–e**). Importantly, the expression of *SOX7* mRNA (expressed in the extra-embryonic endoderm but not the definitive endoderm) was downregulated (Figure 2g,h). These results indicate that the definitive endoderm is induced or selected from human ESCs and iPSCs after passaging. We obtained the same results using another human iPSC line (**Supplementary Figure S2a–d**).

HEX induces hepatoblasts from the human ESC- and iPSC-derived definitive endoderms

To investigate whether forced expression of transcription factors could promote hepatic differentiation, the human ESC- and iPSC-derived definitive endoderms were transduced with Ad vectors. We used a fiber-modified Ad vector containing the elongation factor-1α promoter and a stretch of lysine residue (K7) peptides in the C-terminal region of the fiber knob to examine the transduction efficiency in the human ESC- and iPSC-derived definitive endoderms. The elongation factor-1α promoter was found to be highly active in human ESCs.[28] The K7 peptide targets heparan sulfates on the cellular surface, and the fiber-modified Ad vector containing K7 peptides was shown to be efficient for transduction into many kinds of cells.[29,30] The human ESC- and iPSC-derived definitive endoderms were transduced with a LacZ-expressing Ad vector (Ad-LacZ) at 3,000 vector particle/cell. X-Gal staining showed that the Ad-LacZ-transduced human ESC- and iPSC-derived definitive endoderms successfully expressed LacZ (Figure 3). Nearly 100% of the cells transduced with Ad-LacZ were strongly X-gal positive. The transduction efficiency in the human ESC- and iPSC-derived definitive endoderms transduced with the conventional Ad vector containing the wild-type capsid at 3,000 vector particle/cell was ~80% and X-gal staining was much weaker than that in the cells transduced with fiber-modified Ad vectors (**Supplementary Figure S6**).

Next, the human ESC- and iPSC-derived definitive endoderms were transduced with a HEX-expressing fiber-modified Ad vector (Ad-HEX). Although HEX is known to be a transcription factor that is essential for liver development, it remains unclear what the effect of transient *HEX* overexpression is on differentiation from human ESCs and iPSCs or their derivatives *in vitro*. We confirmed the overexpression of *HEX* in the human ESC- and iPSC-derived definitive endoderms transduced with Ad-HEX (**Supplementary Figure S3a–f**). Gene expression analysis revealed the upregulation of *AFP* mRNA, which was expressed by hepatoblasts or early hepatocytes, in Ad-HEX-transduced cells as